



UNIVERSITÀ
DEGLI STUDI
DI PADOVA



DIPARTIMENTO DI INGEGNERIA DELL'INFORMAZIONE

CORSO DI LAUREA MAGISTRALE IN BIOINGEGNERIA

“Forward dynamic simulation of walking in persons with muscle weakness after incomplete spinal cord injury”

Relatore: Prof. ZIMI SAWACHA

Correlatore: Prof. LANIE GUTIERREZ

Laureanda: GIULIA STOPPA

ANNO ACCADEMICO 2023 – 2024

Data di laurea 9/07/2024

A Giulia Cecchettin,

per ricordare a tutti che l'ingegneria è anche donna.

Stiamo realizzando i tuoi sogni.

Alla mia famiglia, che mi ha sostenuta, abbracciata, spronata. Siete le colonne della mia vita.

Mamma, Papà. Non credo di poter mai riuscire a darvi indietro tutto quello mi avete dato voi in questi anni ma spero che questo mio e nostro traguardo possa essere la prova del mio sforzo per ripagarvi.

Alle mie sorelle. Fede, mi hai insegnato che il mondo non è così grande. Basta un biglietto di sola andata e qualsiasi ambizione diventa realtà. Se mi sono messa così tanto alla prova andando in Svezia è solo merito tuo. Benny, piccolina di casa ma forse la più saggia. Spero che il tuo futuro sia pieno di soddisfazioni proprio come ti meriti. La tua famiglia è sempre qua per te. Fede, Benny, vi porto nella mia pelle.

A Carlo. Mia luce. Tu che mi hai dato la possibilità di inseguire i miei sogni, stando sempre al mio fianco. A te che mi ascolti, non giudichi, mi consigli. La tua presenza costante e la tua pazienza infinita sono stati la mia forza. Spero di essere sempre alla tua altezza.

A tutte le mie amiche. Le mie risate più sincere sono state per voi. Ognuna di voi ha un posto speciale nel mio cuore. Siete la mia famiglia scelta.

A Fausto, Filippo e Federico. La mia famiglia di Padova. Più che coinquilini, fratelli. Voi che mi avete fatto trascorrere i due anni più belli, trasformando tutto in gioco e insegnandomi a vivere con spensieratezza.

A Padova, città del mio cuore. I tuoi angoli mi hanno rapita. Le tue luci mi fanno sentire a casa. È qui che ho trovato amicizia, amore, casa. Mi hai fatta diventare adulta. Rimarrai sempre parte di me.

A tutti voi dico grazie con il cuore. Oggi sono qui grazie voi.

INDEX

ABSTRACT.....	7
ABSTRACT.....	9
Chapter 1 - Introduction: Gait cycle analysis	11
1.1 Gait cycle phases.....	11
1.1.1 Stance phase	11
1.1.2 Swing phase.....	12
1.2 Gait in pathology: focus on spinal cord injury.....	12
Chapter 2 – Spinal Cord Injury.....	15
2.1 Innervation of lower limb muscles.....	17
2.2 Functions affected by lumbar SCI.....	18
2.3 Gait in pathology.....	19
Chapter 3 – Gait simulation and modelling.....	21
3.1 OpenSim.....	21
3.2 Forward VS Inverse simulation.....	22
3.3 Limitations of inverse simulation of walking	25
3.4 Predictive simulations	26
3.5 Multi-terms objective function.....	27
Chapter 4 – Methods.....	29
4.1 Model	29
4.2 Muscle weakness level.....	30
4.3 Predictive simulation framework	31
4.3.1 Cost function	31
4.3.2 Predictive simulation constraints.....	32
Chapter 5 – Results.....	33
5.1 Gait phases duration and objective values evaluation.....	33

5.1.1 S2 SCI simulation	34
5.1.2 S1 SCI simulation	35
5.1.3 L5 SCI simulation	36
5.1.4 L4 SCI simulation	37
5.1.5 L3 SCI simulation	38
5.1.6 L2 SCI simulation	39
5.2 CASE 1: SS 90% - WS 10%.....	40
5.2.1 Joint angles.....	40
5.2.2 Ground reaction force	41
5.2.3 Muscle activations	42
5.3 CASE 2: SS 50% - WS 10%.....	54
5.3.1 Joint angles.....	54
5.3.2 Ground reaction force	55
5.3.3 Muscle activation	56
Chapter 6 – Discussion of results	67
6.1 Objective value evaluation	67
6.2 Gait phases duration	68
6.3 CASE 1: SS 90% - WS 10%.....	68
6.4 CASE 2: SS 50% - WS 10%.....	70
Chapter 7 – Conclusions and limitations of the study.....	73
7.1 Conclusions	73
7.2 Limitations.....	74
Bibliography.....	77

ABSTRACT

Comprendere le complessità del movimento umano è fondamentale nel campo della biomeccanica.

In questo studio, ho esplorato le complessità dei modelli di movimento umano e dei loro risultati biomeccanici. In particolare, ho orientato la mia attenzione verso l'esame di queste dinamiche nel contesto della debolezza muscolare. Il movimento umano è un fenomeno influenzato da molti fattori, e la debolezza muscolare rappresenta un aspetto significativo che può alterare profondamente i modelli di movimento e le risposte biomeccaniche.

Studiando quest'area, ho cercato di capire le complessità associate a come la debolezza muscolare si manifesta e influisce su vari parametri biomeccanici, come la cinematica, i modelli di attivazione muscolare e l'efficienza generale del movimento.

Questa indagine ha comportato uno studio delle simulazioni di camminata sia di individui sani che individui affetti lesione del midollo spinale (SCI), consentendo un'analisi comparativa per chiarire le diverse biomeccaniche associate alla debolezza muscolare.

Approfondirò anche il tema delle simulazioni dinamiche predittive, illustrando le metodologie impiegate e sottolineandone l'importanza nella ricerca biomeccanica. Descriverò le complessità procedurali coinvolte nella conduzione di simulazioni dinamiche, inclusa l'integrazione di modelli muscolo-scheletrici e algoritmi computazionali. In queste simulazioni, ho valutato gli angoli articolari, le forze di reazione al suolo e attivazioni muscolari in varie condizioni.

Analizzando questi parametri, ho cercato di fornire una comprensione completa delle risposte biomeccaniche a diversi livelli di debolezza muscolare e gravità dell'infortunio, evidenziando così gli effetti sfumati sulla dinamica del movimento e sull'efficienza. Lo studio rivela che le simulazioni possono essere raggruppate in tre macro-categorie.

In seguito all'analisi dei modelli di movimento, una fase secondaria dello studio sarà dedicata alla valutazione dei valori obiettivi derivati da ciascuna simulazione. Lo studio del valore obiettivo rivela due tendenze: la diminuzione della debolezza muscolare porta ad un aumento del valore obiettivo, indicando una ridotta efficienza metabolica. Questi risultati evidenziano la relazione tra debolezza muscolare, gravità delle lesioni e efficienza metabolica nelle simulazioni biomeccaniche.

In seguito approfondisco la variazione della durata delle fasi del ciclo del passo. Questa analisi mira a rivelare come la debolezza muscolare influenza gli aspetti temporali del ciclo dell'andatura, facendo luce sulle potenziali alterazioni nei modelli di movimento. Esaminando la durata del ciclo del passo, miro a quantificare l'impatto della debolezza muscolare su questi fattori biomeccanici fondamentali.

Lo studio trova che la velocità fissa induce il modello a regolare le sottofasi del ciclo del passo in risposta ai vari livelli di debolezza muscolare. L'aumento della gravità del SCI e l'asimmetria di debolezza muscolare riducono significativamente la percentuale della fase di supporto singolo, con casi gravi che mostrano una fase di appoggio estesa.

I risultati collettivi di queste fasi contribuiranno non solo all'avanzamento della biomeccanica, ma anche al perfezionamento dei modelli di simulazione dinamica in avanti. Inoltre, le osservazioni acquisite avranno implicazioni per vari campi come la scienza dello sport, la riabilitazione e l'ergonomia, fornendo una prospettiva completa sull'interazione tra debolezza muscolare e risultati biomeccanici.

ABSTRACT

Understanding the intricacies of human movement is a fundamental pursuit in the realm of biomechanics.

In this study, I explored the complexities of human motion patterns and their resultant biomechanical outcomes. Specifically, I directed my focus towards examining these dynamics within the context of muscle weakness. Human movement is a multifaceted phenomenon influenced by lots of factors, and muscle weakness represents a significant aspect that can alter movement patterns and biomechanical responses.

By investigating this area, I aimed to understand the complexities associated with how muscle weakness manifests and impacts various biomechanical parameters, such as kinematics, muscle activation patterns, and overall movement efficiency.

This investigation entailed an examination of simulation of both healthy individuals and those affected by Spinal Cord Injury (SCI), allowing for a comparative analysis to elucidate the distinct biomechanical signatures associated with muscle weakness.

I also will delve into the theme of forward dynamic simulations, elucidating the methodologies employed and underscoring their significance in biomechanical research. I will outline the procedural intricacies involved in conducting forward dynamic simulations, including the integration of musculoskeletal models and computational algorithms. In these simulations, I evaluated joint angles, ground reaction forces, and muscle activation patterns across various conditions. The study reveals that the simulations can be grouped into three macro-categories.

By analyzing these parameters, I aimed to provide a comprehensive understanding of the biomechanical responses to different levels of muscle weakness and SCI severity, thus highlighting the effects on movement dynamics and efficiency.

Following the analysis of movement patterns, a secondary phase of the study will be dedicated to evaluating objective values derived from each simulation. The objective value study reveals two trends: decreasing muscle weakness leads to an increase in the objective value, indicating reduced metabolic efficiency. These findings highlight the relationship between muscle weakness, injury severity, and metabolic efficiency in biomechanical simulations.

Then I studied the variation in the duration of the gait cycle. This analysis aims to reveal how muscle weakness influences the temporal aspects of the gait cycle. By examining the duration of the gait cycle, I aim to quantify and understand the impact of muscle weakness on these fundamental biomechanical factors.

The study finds that fixed velocity causes the model to adjust gait cycle subphases in response to varying muscle weakness levels. Increased SCI severity and asymmetric muscle weakness reduce the single support phase percentage, with severe cases showing an extended stance phase.

The collective findings from these stages will contribute not only to the advancement of biomechanics but also to the refinement of forward dynamic simulation models. Additionally, the observations gained will have implications for various fields such as sports science, rehabilitation, and ergonomics, providing a comprehensive perspective on the interplay between muscle weakness and biomechanical outcomes.

Chapter 1 - Introduction: Gait cycle analysis

Gait analysis is a crucial component of biomechanics research ([2], [3]) aimed at understanding human locomotion patterns and their implications for clinical diagnosis, rehabilitation, and athletic performance enhancement. Central to gait analysis is motion analysis, a methodology involving the precise measurement and analysis of movement patterns using advanced tools and techniques.

Motion analysis encompasses the use of various instruments such as high-speed cameras, force plates, inertial measurement units (IMUs), and electromyography (EMG) sensors. These tools enable researchers to capture, record, and analyze the intricate movements of the human body during activities such as walking, running, or jumping.

By leveraging motion analysis, researchers can quantify parameters like joint angles, segmental motion, ground reaction forces, and muscle activation patterns, providing valuable insights into biomechanical principles underlying human locomotion [10]. The integration of motion analysis with gait analysis allows for a comprehensive examination of gait mechanics, facilitating the identification of abnormalities, the assessment of interventions, and the optimization of movement strategies for various populations.

1.1 Gait cycle phases

The gait cycle is typically divided into two main phases: the stance phase and the swing phase. Each of these phases has sub-phases that capture specific events during walking [3].

1.1.1 Stance phase

The stance phase encompasses the period when the foot is in contact with the ground. It consists of several sub-phases:

- Initial Contact (IC): The moment when the foot first contacts the ground.
- Loading Response (LR): The period of weight acceptance as the body weight transfers onto the reference limb.

- Midstance (MSt): The point when the reference limb is directly beneath the body, and the opposite foot is lifted off the ground.
- Terminal Stance (TSt): The phase between midstance and the initial contact of the opposite limb.
- Pre-swing (PSw): The final phase of the stance, preparing for the swing phase.

1.1.2 Swing phase

The swing phase begins when the foot leaves the ground and continues until the next initial contact. Sub-phases include:

- Initial Swing (ISw): The early part of the swing phase.
- Mid-swing (MSw): The midpoint of the swing phase.
- Terminal Swing (TSw): The final phase before the foot prepares for initial contact.

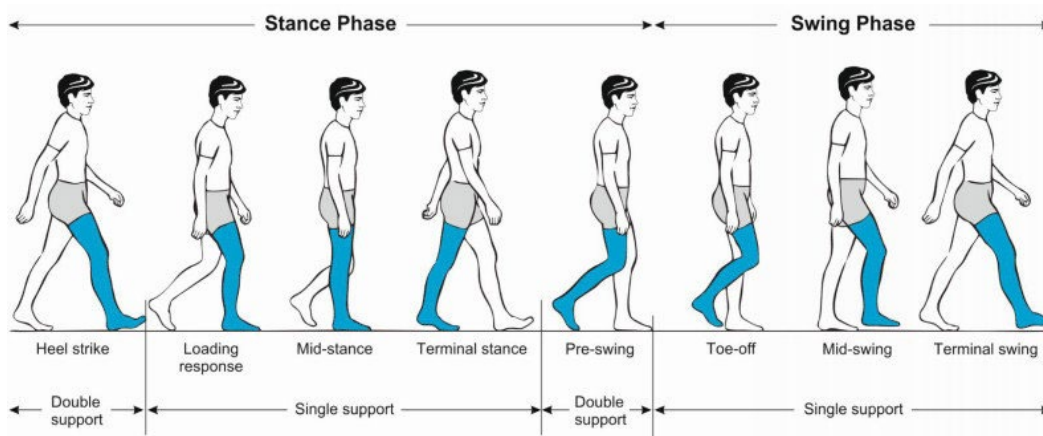


Fig. 1: gait cycle phases, reprinted from [1]

1.2 Gait in pathology: focus on spinal cord injury

Gait analysis in individuals with spinal cord injury (SCI) is a critical area of research with profound implications for rehabilitation and quality of life. SCI can result in significant impairments in motor function, sensation, and coordination, leading to distinct challenges in walking [3]. Understanding the alterations in the gait pattern associated with SCI is crucial for developing effective rehabilitation strategies and assistive technologies.

Spinal cord injury disrupts the normal neural pathways responsible for controlling voluntary movements, including walking [11]. Individuals with SCI often experience muscle weakness, altered muscle tone, and impaired proprioception, which profoundly affect their gait pattern. The extent and location of the spinal cord lesion contribute to the variability in gait impairments among individuals with SCI.

The loss of supraspinal control over lower limb muscles leads to weakness and reduced coordination during walking. This often results in an altered gait pattern characterized by a decreased step length, reduced walking speed, and an increased reliance on upper limb support. Spasticity, a common consequence of SCI, can contribute to abnormal muscle tone during gait. This may manifest as stiff-legged walking, with an increased risk of falls. Managing spasticity becomes crucial in optimizing gait function in individuals with SCI [12].

The loss of sensory input and motor control compromises balance and stability during walking. Individuals with SCI may exhibit an increased variability in step width, an altered center of mass trajectory, and difficulties in weight shifting.

Chapter 2 – Spinal Cord Injury

The human spinal cord, a complex and delicate bundle of nerves, serves as the intricate highway for communication between the brain and the body.

Two primary pathways exist: the ascending, or sensory, pathway carries sensory information from the periphery to the brain, allowing for the perception of touch, temperature, pain, and proprioception [4]. In contrast, the descending, or motor, pathway transmits commands from the brain to the periphery, initiating voluntary muscle movements and coordinating motor responses [5].

However, when this vital pathway is disrupted by trauma, disease, or other unforeseen circumstances, the consequences can be profound.

A spinal cord injury (SCI) is a traumatic condition that affects the spinal cord, a crucial part of the central nervous system. The spinal cord plays a vital role in transmitting messages between the brain and the rest of the body, controlling various bodily functions and movements. When the spinal cord is damaged, it can lead to a range of disabilities and challenges.

SCI can result from various causes, including traumatic cases as car crashes, falls, or sports injuries and non-traumatic cases as disease (spinal cord tumors, degenerative disorders), infections as meningitis or polio and ischemia (lack of blood supply to the spinal cord can cause ischemic injury).

Spinal cord injuries are categorized based on the extent of damage and the resulting impact on sensory and motor functions. These classifications are crucial in understanding the prognosis and planning appropriate interventions for individuals with SCI.

Fig. 2: AIS Worksheet, reprinted from [6]

The ASIA Impairment Scale (AIS) developed by the American Spinal Injury Association (ASIA) (Fig. 2) is widely recommended to classify the severity of injury [6] [7]. The scale has five classification levels, ranging from complete loss of neural function in the affected area to completely normal. The results help the team set functional goals based on the neurological level of injury that is determined.

Elements of the scale, according to the National Institutes of Health, include:

Grade A: The impairment is complete. There is no motor or sensory function left below the level of injury.

Grade B: The impairment is incomplete. Sensory function, but not motor function, is preserved below the neurologic level (the first normal level above the level of injury) and some sensation is preserved in the sacral segments S4 and S5.

Grade C: The impairment is incomplete. Motor function is preserved below the neurologic level, but more than half of the key muscles below the neurologic level have a muscle grade less than 3 (i.e., they are not strong enough to move against gravity).

Grade D: The impairment is incomplete. Motor function is preserved below the neurologic level, and at least half of the key muscles below the neurologic level have a muscle grade of 3 or more (i.e., the joints can be moved against gravity).

Grade E: The patient's functions are normal. All motor and sensory functions are unhindered.

2.1 Innervation of lower limb muscles

Nerve segmentation is a fundamental concept in the anatomy and physiology of the nervous system. This concept is based on the idea that the spine is divided into segments, each of which is associated with a specific level. These segments correspond to the spinal nerves that emerge from the spine and are responsible for the innervation of specific regions of the body.

The human spine is composed of vertebrae, and each of these vertebrae is associated with a particular level or segment. There are eight cervical nerves (C1-C8) in the neck region, twelve thoracic nerves (T1-T12) in the thoracic region, five lumbar nerves (L1-L5) in the lumbar region, five sacral nerves (S1-S5) in the sacral region, and one coccygeal nerve (Co) in the coccygeal region.

These spinal nerves carry nerve impulses to and from the spinal cord, which in turn communicates with the brain. Each spinal nerve is associated with a specific dermatome, representing the area of skin innervated by that nerve. Additionally, each nerve provides motor and sensory innervation to specific groups of muscles and parts of the body [8].

The concept of nerve segmentation, as outlined in the discussion above, plays a pivotal role in understanding the intricate innervation patterns of the human body. In 1964, Sharrard contributed significantly to this field through a paper titled "The segmental innervation of the lower limb muscles in man" [13]. In this work, Sharrard likely delved into the detailed schematization of the innervation of lower limb muscles, exploring how specific segments of the spinal column correspond to the motor and sensory functions of various muscles in the legs. This seminal paper would likely have provided valuable insights into the segmental organization of the nervous system, elucidating the precise connections between spinal nerves and the lower limb musculature.

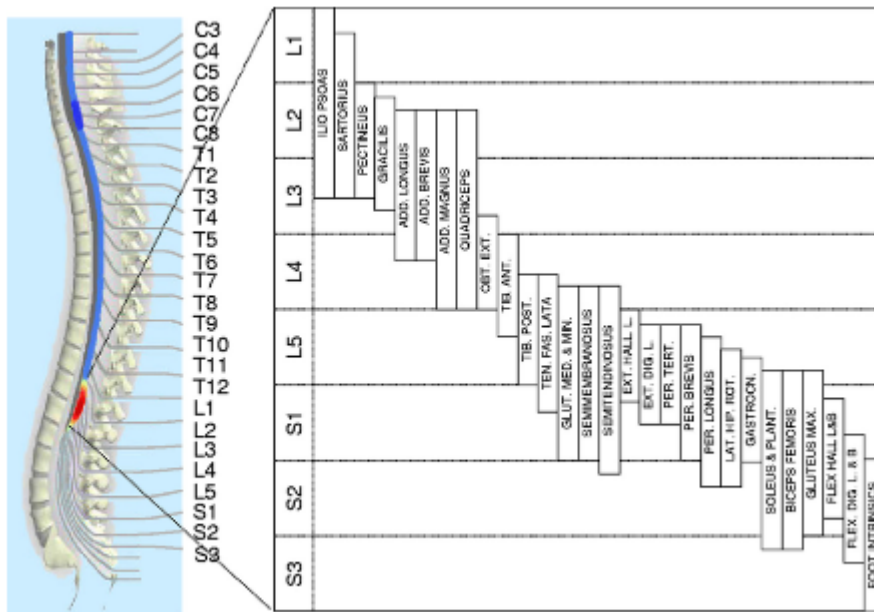


Figure 3: Innervation of lower limb muscles (adapted from[13])

2.2 Functions affected by lumbar SCI

The level of SCI refers to the lowest level of the spinal cord in which sensory and motor functions remain intact. Medical professionals often use the International Standards for Neurological Classification to determine the level of SCI. This involves testing sensation and motor functions in various areas of the body.

The following summary list explains which functions may be affected at each level of lumbar SCI [7].

Lumbar Nerves (L1 – L5):

- Injuries generally result in some loss of function in the hips and legs;
- Little or no voluntary control of bowel or bladder, but can manage on their own with special equipment;
- Depending on strength in the legs, may need a wheelchair and may also walk with braces.
- Sacral Nerves (S1-S5):
- Injuries generally result in some loss of function the hips and legs;
- Little or no voluntary control of bowel or bladder, but can manage on their own with special equipment;
- Most likely will be able to walk.

2.3 Gait in pathology

Gait analysis assumes particular significance in the context of SCI, where disruptions to the spinal cord comprise the intricate neural pathways responsible for coordinated movement. Following an SCI, alterations in gait become a prominent feature, reflecting the profound impact on motor function and mobility. Individuals with SCI often exhibit changes in their walking pattern, characterized by challenges in balance, muscle control, and coordination. Gait abnormalities may include a shortened stride length, altered walking speed, or an asymmetrical gait pattern [9].

The extent and nature of these alterations depend on the level and severity of the SCI.

Here are some common alterations in gait observed in individuals with SCI [14]:

- Maintaining balance becomes more challenging after an SCI. The disruption of neural pathways can lead to difficulties in weight shifting and stability during walking;
- SCI can affect the control of muscles and coordination necessary for smooth and coordinated movements during walking. This may result in an unsteady or uneven gait;
- Individuals with SCI may exhibit a shortened stride length. The ability to take long steps might be compromised, affecting the overall efficiency and speed of walking;
- The speed of walking can be affected, with individuals often walking more slowly than before the injury. The extent of this change varies depending on the severity and level of the SCI;
- An SCI can lead to an asymmetrical gait pattern, where there is an imbalance or inconsistency in the movement of the limbs. This can result from muscle weakness or spasticity on one side of the body.

Chapter 3 – Gait simulation and modelling

Understanding the intricacies of the gait cycle is crucial in various fields such as biomechanics, rehabilitation, and sports science. Simulation and modeling play a pivotal role in this exploration by providing a controlled environment to analyze and comprehend the complex dynamics of human locomotion.

Through the utilization of mathematical models and computational simulations, researchers can simulate different scenarios, alter parameters, and observe the resulting changes in the gait cycle. This not only enhances our theoretical understanding of the biomechanics involved but also allows for the exploration of diverse physiological conditions and potential interventions. Moreover, simulation facilitates the analysis of subtle nuances in gait patterns that may be challenging to capture in real-world experiments alone.

In essence, simulation and modeling serve as powerful tools for unraveling the intricacies of the gait cycle, contributing significantly to advancements in biomechanical research and the development of targeted interventions for gait-related disorders [3].

3.1 OpenSim

This comprehensive tool enables researchers to create detailed models of the human body, including bones, muscles, ligaments, and joints, based on medical imaging data such as MRI or CT scans. Through OpenSim's intuitive interface, users can customize and refine these models to accurately represent individual anatomy and biomechanics [10].

The OpenSim pipeline encompasses several stages, from the acquisition of data to the analysis of kinematics and kinetics.

1. OpenSim model: represents the dynamics of a system of rigid bodies and joints that are acted upon by forces to produce motion. The OpenSim model file is made up of components corresponding to parts of the physical system. These parts include bodies, joints, forces, constraints, and controllers;
2. Scaling: the aim of scaling a generic musculoskeletal model is to modify the anthropometry, or physical dimensions, of the generic model so that it matches the anthropometry of a particular subject. In OpenSim, the scaling step adjusts both the

mass properties (mass and inertia tensor), as well as the dimensions of the body segments.

3. Inverse Kinematics (IK): Once the model is constructed, OpenSim finds the set of generalized coordinates (joint angles and positions) for the model that best match the experimental kinematics recorded for a particular subject. The IK tool goes through each time step of motion and computes generalized coordinate values which positions the model in a pose that “best matches” experimental markers and coordinate values for that time step. Mathematically, the “best match” is expressed as a weighted least squares problem, whose solution aims to minimize both marker and coordinate errors.
4. Inverse Dynamics (ID): The Inverse Dynamics (ID) tool determines the generalized forces (e.g., net forces and torques) that cause a particular motion, and its results can be used to infer how muscles are utilized for that motion. To determine these internal forces and moments, the equations of motion for the system are solved with external forces (e.g., ground reactions forces) and accelerations given (estimated by differentiating angles and positions twice).

Overall, the OpenSim pipeline [15] offers a systematic approach for analyzing human movement, providing insights into the complex interactions between anatomy, biomechanics, and motor control.

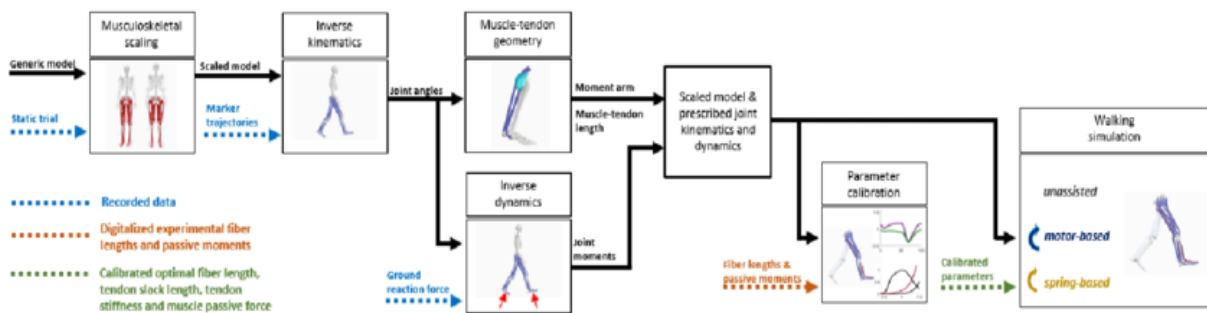


Fig. 5: OpenSim pipeline

3.2 Forward VS Inverse simulation

The human body performs tasks through neural commands from the central nervous system (CNS). Biomechanical analyses involve a dynamic formulation derived from a workflow, as depicted in Figure 4, illustrating the path from neural commands to specific postures and vice versa.

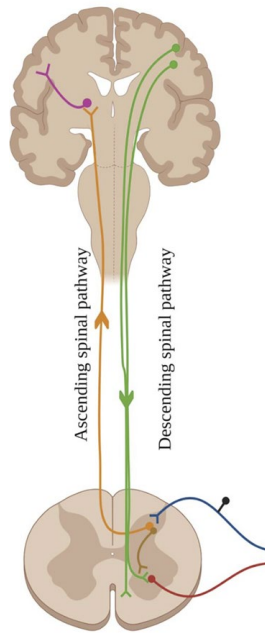


Fig. 4: Ascending and descending spinal pathway

This dynamic formulation can be either explicitly or implicitly represented. In explicit dynamic formulation, system dynamics are directly integrated or differentiated, while in implicit dynamic formulation, system dynamics are considered as constraint equations implicitly satisfied within an optimization-based simulation.

Explicit dynamic formulation includes forward inverse, and mixed approaches. Forward approaches, the one which will be used in this study, involve receiving neural commands to generate muscle excitations, which drive muscle activation dynamics. Muscle contraction dynamics are modeled using first-order differential equations and Hill-type muscle models (*Fig. 7*) to convert muscle activations to forces.

Musculoskeletal geometry, incorporating muscle attachment sites, lines of actions, wrapping points, surfaces, and moment arms, is used to calculate joint moments, influencing skeletal motion dynamics solved through numerical integration.

Inverse approaches, on the other hand, use posture/motion to determine neural commands. Physiologically meaningful values for neural commands, muscle activation dynamics, and muscle contraction dynamics are crucial for accurate estimations.

Mixed approaches in explicit dynamic formulations leverage the best features of both forward and inverse dynamics approaches.

	FORWARD SIMULATION	INVERSE SIMULATION
DESCRIPTION	The biomechanical system is driven by input forces or muscle activations, and the resulting motion of the skeletal system is calculated over time	The objective is to determine the muscle activations or forces required to produce a specific observed motion or desired outcome
USE CASES	<ul style="list-style-type: none"> – Understanding how external force of muscle activations influence the motion of the musculoskeletal system; – Rehabilitation planning <p>where the goal is to predict the motion of a person under certain conditions or interventions.</p>	<ul style="list-style-type: none"> – Clinical setting to estimate muscle force or activations based on observed gait patterns to understand gait patterns; – Design prosthetics by understanding the forces required to mimic natural gait patterns

Table 1: Forwards simulation vs Inverse simulation summary

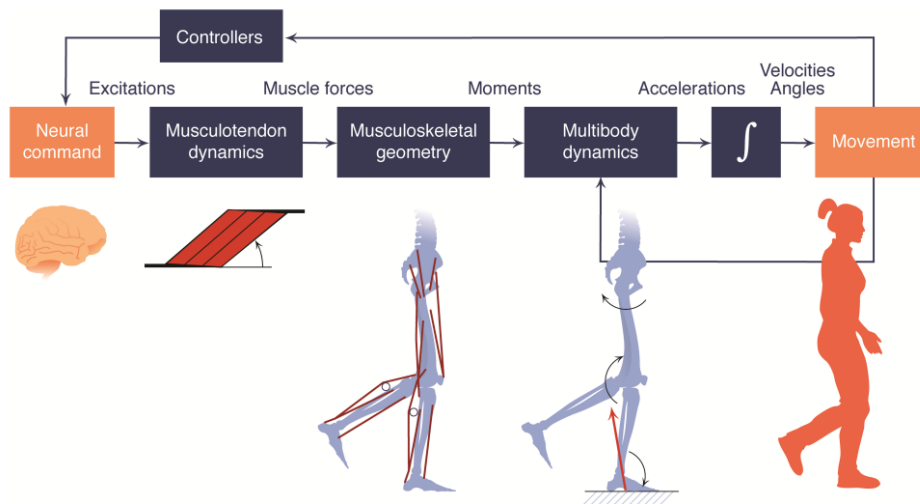


Fig. 5: Elements of a typical forward dynamic simulation in OpenSim. Reprinted from [16]

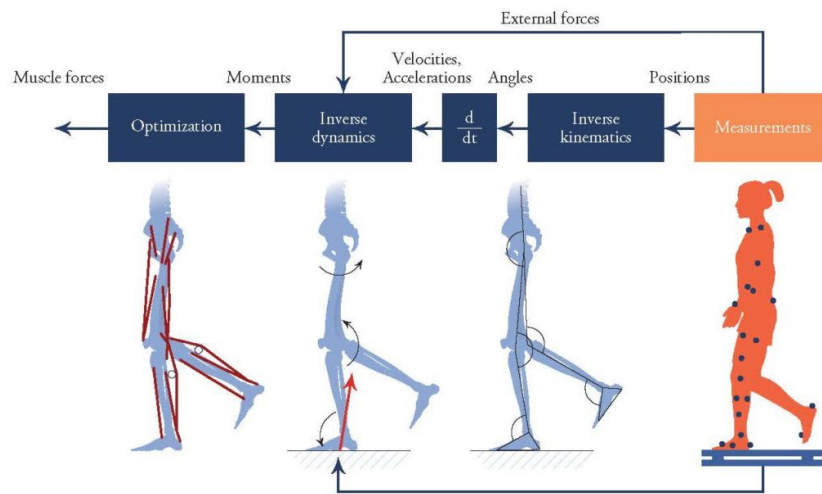


Fig. 6: Elements of a typical inverse dynamic analysis in OpenSim. Reprinted from [16]

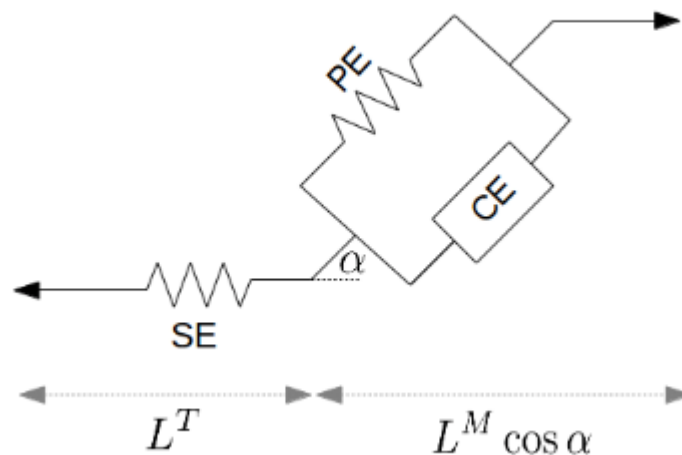


Fig. 7: Hill's muscle model. SE: elastic component or series elastic element, PE: contractile elements in parallel, CE: contractile elements in series, α : pennation angle, L^T : total reference length, L^M : muscle length.

3.3 Limitations of inverse simulation of walking

Inverse simulations of walking offer valuable insights into human biomechanics, providing a non-invasive means to study locomotion. However, the methodology is not without its limitations, particularly when it comes to the challenge of obtaining precise measurements from patients.

This chapter explores the inherent difficulties in acquiring comprehensive data directly from individuals due to the invasiveness of certain measurement techniques, leading to necessary approximations in inverse simulations.

One significant limitation stems from the fact that obtaining certain crucial biomechanical measurements directly from patients can be overly invasive. In clinical settings some measurements involving internal structures or sensitive areas might not be ethically or practically feasible to collect [16]. For instance, direct measurements of muscle forces, joint torques, or detailed kinematics often require invasive procedures, such as implanting sensors or conducting muscle biopsies. These procedures pose risks, discomfort, and ethical considerations that limit the extent to which comprehensive data can be directly obtained from patients.

By employing forward gait simulations, researchers can circumvent the challenges associated with invasive measurements, providing a pathway to a more profound comprehension of human locomotion.

3.4 Predictive simulations

Predictive forward simulations in biomechanics and gait analysis have several advantages [17]:

- **Causal Understanding:** Forward simulations allow researchers to investigate the causal relationship between inputs (e.g., muscle activations, external forces) and outputs (e.g., joint movements, ground reaction forces). This helps in gaining a deep understanding of how biomechanical factors contribute to observed motions;
- **Intervention Planning:** Forward simulations are useful for predicting the effects of interventions or changes in muscle activations. This is particularly valuable in rehabilitation planning, where clinicians can simulate the impact of different exercises or treatments on the patient's biomechanics.
- **Realistic Motion Representation:** Forward simulations produce realistic motion patterns, considering the complex interactions between muscles, joints, and external forces. This provides a more accurate representation of human movement compared to simplified models.

- **Biomechanical Research:** Researchers can use forward simulations to explore various scenarios, test hypotheses, and contribute to the development of biomechanical theories. This aids in advancing the overall understanding of human movement.
- **Muscle Function Analysis:** Forward simulations provide insights into how different muscles contribute to specific movements. This information is crucial for understanding muscle function, identifying synergies between muscles, and designing targeted interventions.

3.5 Multi-terms objective function

In the context of optimization and machine learning, a multi-term cost function (or multi-objective function) is a function that combines multiple objectives, often conflicting with each other, into a single optimization criterion. Weights in a multi-term cost function play a crucial role in balancing the relative importance of each term (or objective) within the overall cost function.

The weights need for:

- Weights help determine how much each objective contributes to the overall optimization criterion, allowing the model to find a compromise between these conflicting objectives.
- By assigning different weights, one can prioritize certain objectives over others, directly influencing the outcome of the optimization. This is particularly useful when some objectives are considered more important or desirable in specific applications or contexts.

Assigning a high weight to a term in the cost function means that the corresponding objective is deemed very important. During the optimization process, the model will primarily strive to satisfy this objective, even at the expense of others. In practice, this could mean significantly reducing the error on a training dataset but risking increased model complexity (and potentially overfitting).

Conversely, assigning a low weight indicates that the corresponding objective is considered less critical. This objective will have a lesser impact on the overall optimization, allowing the model to more easily compromise on this aspect to achieve

improvements on other fronts. This could translate into less emphasis on error reduction in favor of better generalization or model simplicity.

Choosing weights in a multi-term cost function is thus a key aspect that requires careful consideration, as it directly influences the balance between optimization objectives and determines the properties and performance of the resulting model. This is the reason why I choose to maintain the default setting of the weights [\[18\]](#).

Chapter 4 – Methods

4.1 Model

To perform the simulations an OpenSim musculoskeletal model ‘Hamner’ has been used [23] [24].

This has:

- 31 degrees of freedom (DoFs) pelvis-to-ground: 6 DoFs, hip: 3 DoFs, knee: 1 DoF, ankle: 1 DoF, subtalar: 1 DoF, metatarsophalangeal-toe: 1 DoF, lumbar: 3 DoFs, shoulder: 3 DoFs, and elbow: 1 DoF);
- 12 segments (calcaneus and toes counted as one segment);
- 92 muscles actuating the lower limb and lumbar joints;
- 8 ideal torque motors actuating the shoulder and elbow joints;
- 6 contact spheres per foot (stiffness of the sphere: 1 N/m²).

A physiologically plausible model of the feet, incorporating toe joints, not only enhances the robust elicitation of knee flexion during stance but also improves ankle kinetics in stance while reducing the overestimation of the initial vertical ground reaction force peak [19] [20].

Each muscle in the model is represented as a Hill-type muscle-tendon unit (Fig. 7).

Muscle groups	Muscles
Harmstrings	Biceps femoris short head
	Biceps Femoris long head
	Semimebranosus
	Smitendinosus
Plantarflexors	Gastrocnemius Medial
	Gastrocnemius Lateral
	Soleus
Quadriceps	Rectus femoris
	Vasti Lateralis
	Vasti Medialis
	Vasti Intermedius
	Gluteus Maximus
	Gluteus Medius
	Iliacus
Tibialis Anterior	

Table 2: Hamner's model muscles

4.2 Muscle weakness level

Based on Sharrard’s proposed schema of segmental innervation of lower limb muscles I examined 36 cases representing different levels of severity of spinal cord injuries for each SCI level between L2 and S2. For each injury level, I conducted simulations across 6 distinct severity grades, progressively reducing the maximum isometric strength of the muscles innervated by involved muscles.

I simulated both symmetric SCI (both the right and left legs have muscles weakened by the same percentage) as simulation number 1 and 6 in the table below, and asymmetric SCI (I simulated left leg stronger than right leg) but my focus are asymmetric ones to evaluate the compensatory strategy of the muscles in the strongest side.

Here there is a table that summarizes the simulations I did (Table 3).

SIMULATION NUMBER	INJURY LEVEL	MUSCLES INVOLVED	MAX ISOMETRIC MUSCLE FORCE
1	S2	Gluteus maximus Biceps femoris Soleus	Left side: 90% Right side: 90%
2	S2	Gluteus maximus Biceps femoris Soleus	Left side: 90% Right side: 50%
3	S2	Gluteus maximus Biceps femoris Soleus	Left side: 90% Right side: 10%
4	S2	Gluteus maximus Biceps femoris Soleus	Left side: 50% Right side: 50%
5	S2	Gluteus maximus Biceps femoris Soleus	Left side: 50% Right side: 10%
6	S2	Gluteus	Left side: 10%

		maximus Biceps femoris Soleus	Right side: 10%
--	--	-------------------------------------	-----------------

This table summarizes the simulations conducted for the S2 level of SCI, emphasizing the calculated percentages of muscle strength reduction.

Each simulation scenario is designed to offer insights into the varying degrees of impairment associated with S2 level injuries, facilitating a better understanding of the potential impacts on muscle functionality.

The same analysis has been conducted also for S1, L5, L4, L3, and L2 levels, focusing on the reduction of muscle strength in the muscles affected by the injury, following the scheme proposed in Fig. 3.2.

4.3 Predictive simulation framework

I formulated predictive simulations of walking as optimal control problems. I used the code developed by Falisse et al. to generate three-dimensional muscle-driven predictive simulations of human gait. [20] [21].

4.3.1 Cost function

Cost function included metabolic energy rate, muscle activity, joint accelerations, passive torques, and excitations of the ideal torque motors at the arm joints.

$$J = \frac{1}{d} \int_0^{t_f} (w_1 \dot{E}^2 + w_2 a^2 + w_3 u_a^2 + w_4 T_p^2 + w_5 e_a^2) dx$$

where d is distance traveled by the pelvis in the forward direction, t_f is half gait cycle duration, a are muscle activations, u_a are accelerations of the lower limb and lumbar joint coordinates, T_p are passive torques, e_a are excitations of the ideal torque motors driving the shoulder and elbow joints, t is time, and w are weight factors.

In particular:

- $w1 = 500$
- $w2 = 2000$
- $w3 = 50000$
- $w4 = 1000$
- $w5 = 10^6$

Metabolic energy rate E has been modeled using a smooth approximation of the phenomenological model described by Bhargava et al. [22] which describes metabolic energy rate as the sum of four terms: muscle activation, shortening, and maintenance heat rates, and mechanical work rate.

4.3.2 Predictive simulation constraints

I configured the main code by setting specific constraints in the objective function.

$S.misc.gaitmotion_type = FullGaitCycle$, to simulate a full gait cycle. Simulating a half gait cycle reduces computation time, but is limited to symmetric models.

$S.solver.tol_ipopt = 3$, the power 10^{-3} the tolerance $ipopt$ has to reach before the OCP can be regarded as solved.

$S.solver.max_iter = 2000$, maximum number of iterations after which the solver will stop.

$S.solver.N_meshes = 100$, number of mesh intervals. Falisse et al. found that the dynamic equations were satisfied at 300 collocation points.

$S.solver.v_pelvis_x_trgt = 0.8$, average velocity (meters per second). In a pathological walking simulation, it is advisable to set a low speed so that the simulation can converge to a solution even in the presence of significant disturbances or anomalies related to pathological conditions. By reducing the speed, the model is given more opportunities to adapt and resolve complexities associated with pathological conditions, allowing for a more accurate and stable simulation.

Chapter 5 – Results

5.1 Gait phases duration and objective values evaluation

In this chapter, I present the outcomes derived from all the simulations, focusing on the stance phase of the gait cycle and the objective values of each simulation.

The results will be shown starting from the less severe case (S2 SCI level) to the most severe case (L2 SCI level).

Legend for ‘Gait Phases Duration’ Tables:

DS1 = first double support.

SS = single support.

DS2 = second double support.

NI = not injured.

90 - 90 = both legs have muscles strength reduced to 90% of max isometric force.

90 - 50 = strong leg has muscles strength reduced to 90% of max isometric force and weak leg has muscles strength reduced to 50% of max isometric force.

90 - 10 = strong leg has muscles strength reduced to 90% of max isometric force and weak leg has muscles strength reduced to 10% of max isometric force.

50 - 50 = both legs have muscles strength reduced to 50% of max isometric force.

50 - 10 = strong leg has muscles strength reduced to 50% of max isometric force and weak leg has muscles strength reduced to 10% of max isometric force.

10 - 10 = both legs have muscles strength reduced to 10% of max isometric force.

5.1.1 S2 SCI simulation

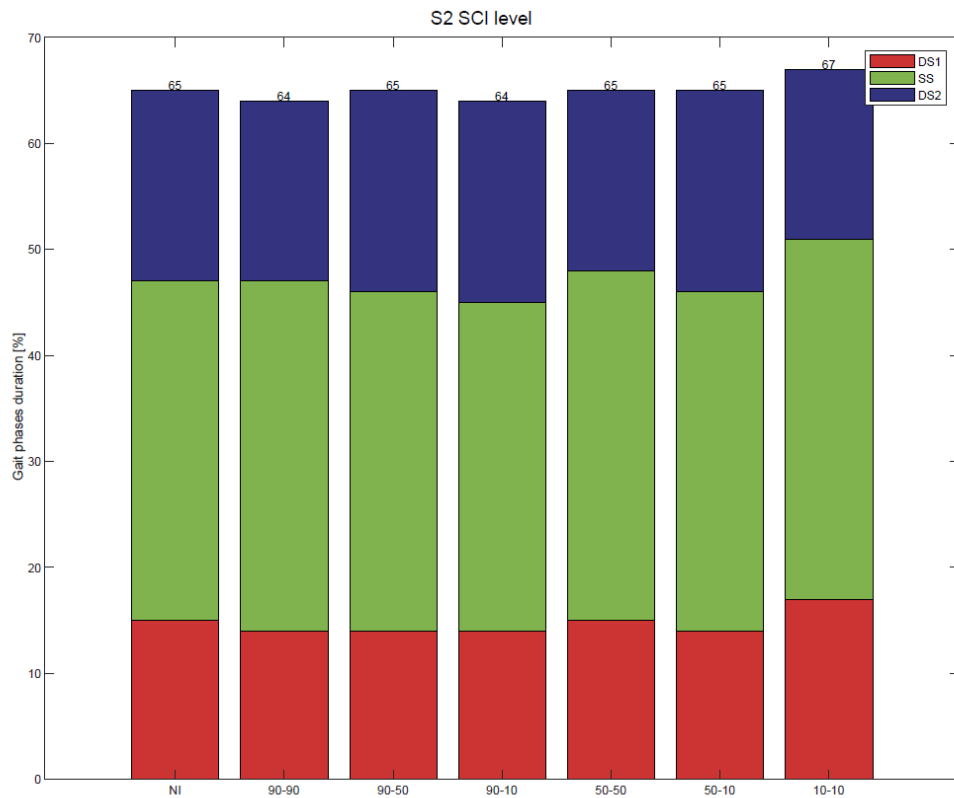


Table 4: Percentage values of gait phases in S2 level of SCI simulation.

	90% SS	50% SS	10% SS
90% WS	2.41E+02	2.42E+02	2.47E+02
50% WS	2.42E+02	2.42E+02	2.47E+02
10% WS	2.47E+02	2.47E+02	2.55E+02

Table 5: Objective values of S2 level of SPI simulation, symmetric table with respect to the diagonal

In 'Not injured' simulation the objective value is 2.43E+02.

5.1.2 S1 SCI simulation

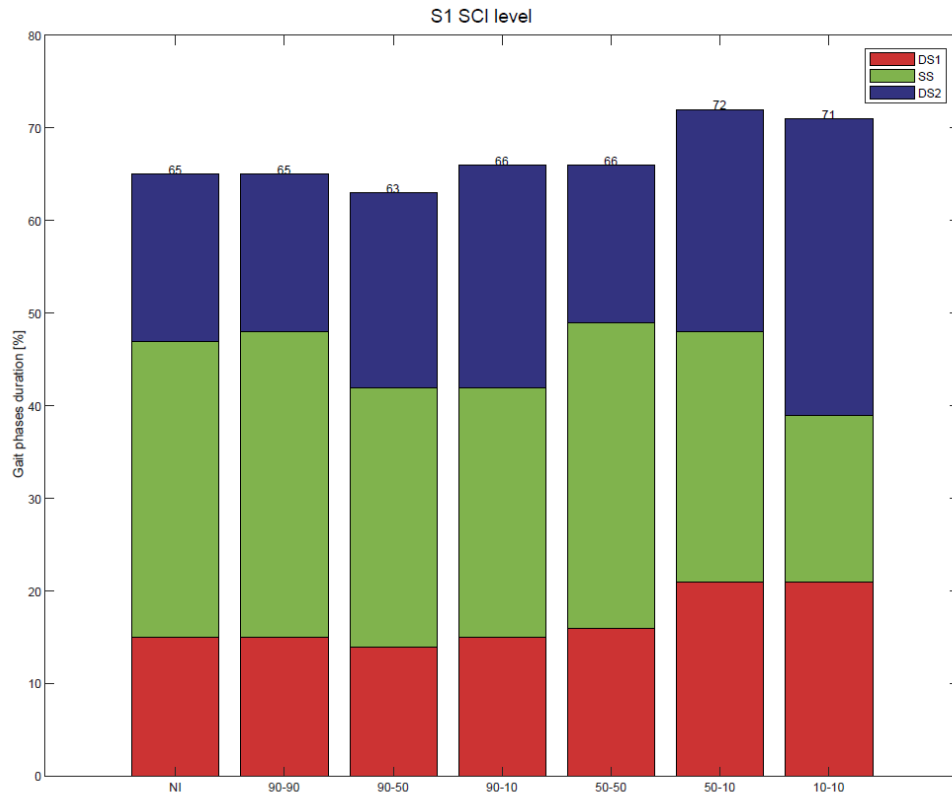


Table 6: Percentage values of gait phases in S1 level of SCI simulation.

	90% SS	50% SS	10% SS
90% WS	2.46E+02	2.71E+02	3.41E+02
50% WS	2.71E+02	3.41E+02	3.94E+02
10% WS	3.41E+02	3.94E+02	4.92E+02

Table 7: Objective values of S1 level of SCI simulation, symmetric table with respect to the diagonal.

5.1.3 L5 SCI simulation

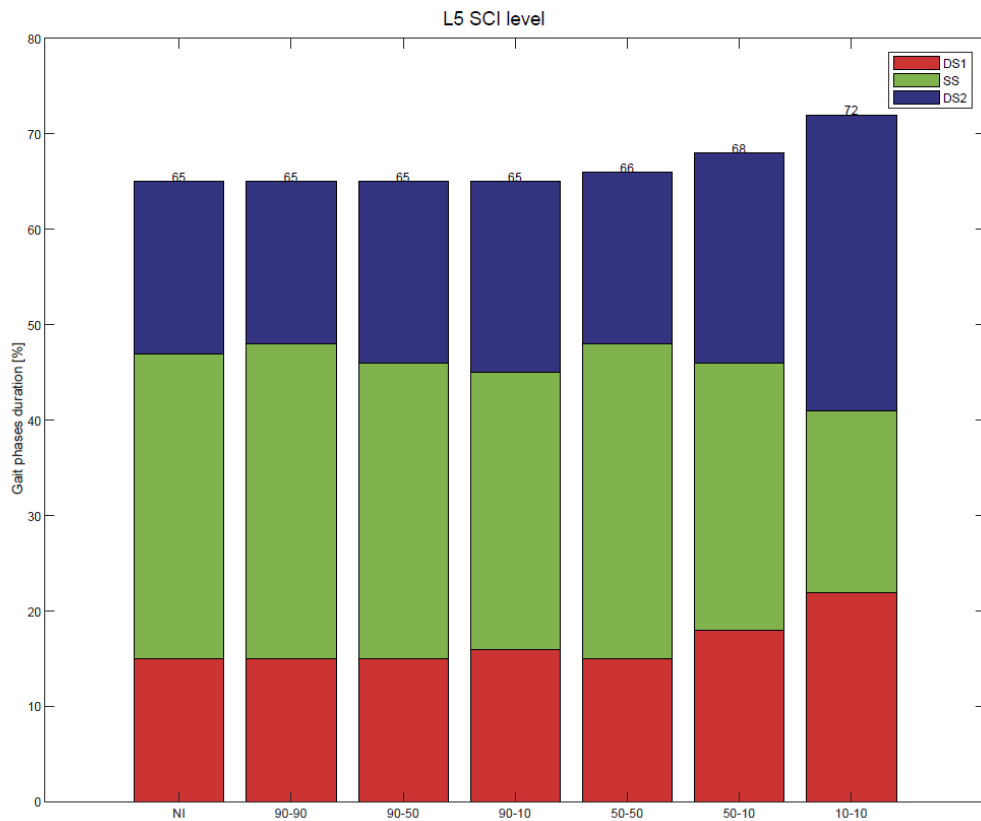


Table 8: Percentage values of gait phases in L5 level of SCI simulation.

	90% SS	50% SS	10% SS
90% WS	2.46E+02	2.46E+02	3.48E+02
50% WS	2.46E+02	3.11E+02	4.08E+02
10% WS	3.48E+02	4.08E+02	5.70E+02

Table 9: Objective values of L5 level of SCI simulation, symmetric table with respect to the diagonal.

5.1.4 L4 SCI simulation

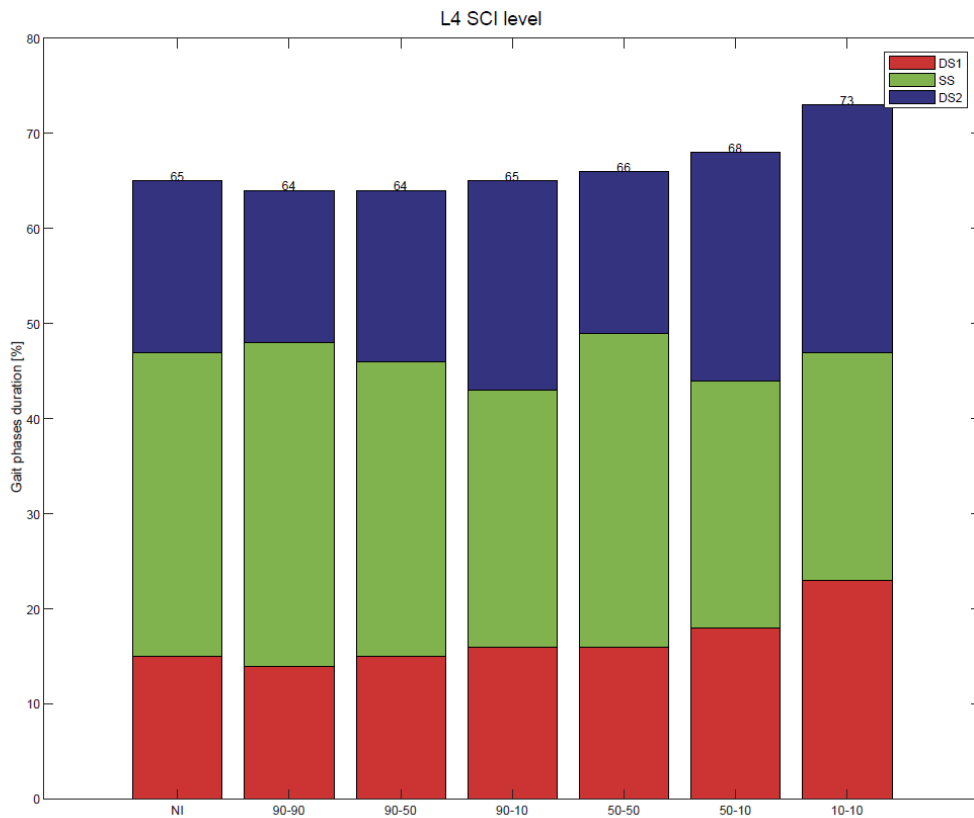


Table 10: Percentage values of gait phases in L4 level of SCI simulation.

	90% SS	50% SS	10% SS
90% WS	2.47E+02	2.73E+02	3.67E+02
50% WS	2.73E+02	3.08E+02	4.32E+02
10% WS	3.67E+02	4.32E+02	7.74E+02

Table 11: Objective values of L4 level of SCI simulation, symmetric table with respect to the diagonal.

5.1.5 L3 SCI simulation

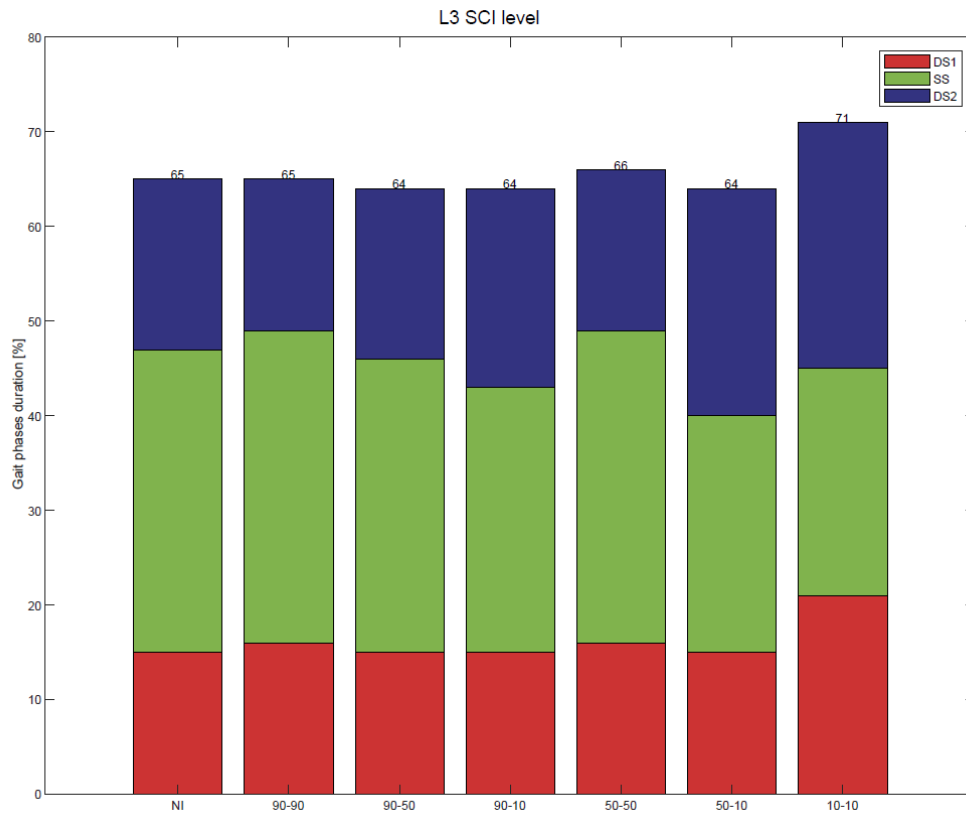


Table 12: Percentage values of gait phases in L3 level of SCI simulation.

	90% SS	50% SS	10% SS
90% WS	2.47E+02	2.73E+02	3.64E+02
50% WS	2.73E+02	3.09E+02	4.33E+02
10% WS	3.64E+02	4.33E+02	8.05E+02

Table 13: Objective values of L3 level of SCI simulation, symmetric table with respect to the diagonal.

5.1.6 L2 SCI simulation

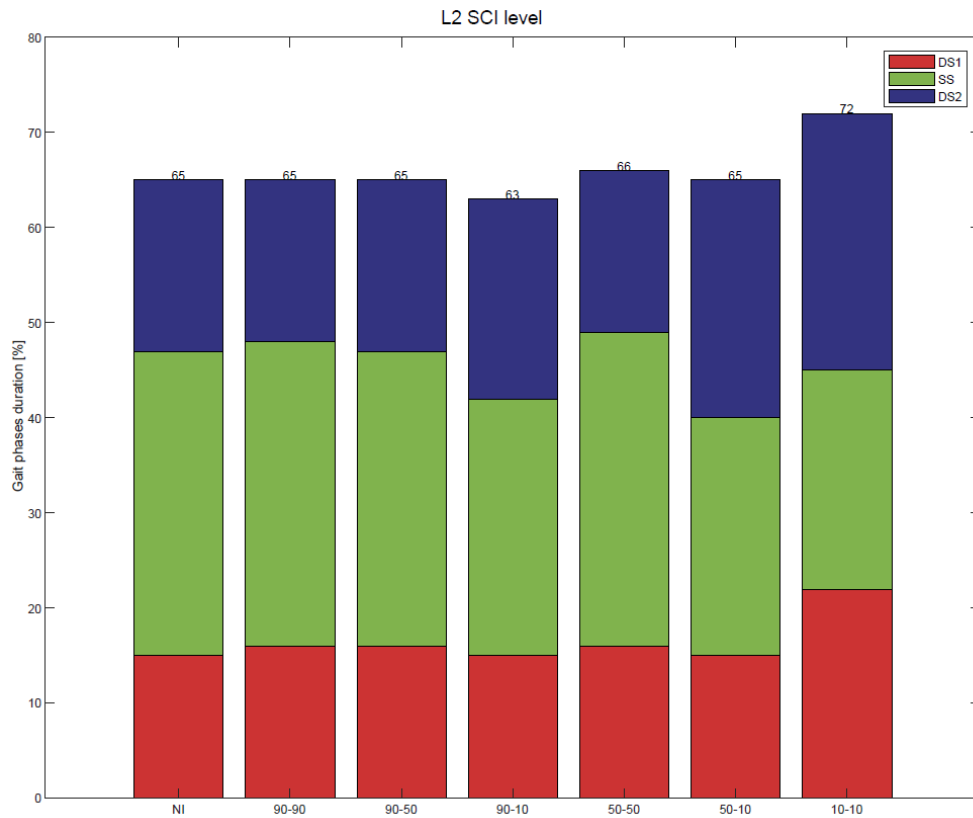


Table 14: Percentage values of gait phases in L2 level of SCI simulation.

	90% SS	50% SS	10% SS
90% WS	2.47E+02	2.74E+02	3.54E+02
50% WS	2.74E+02	3.10E+02	4.21E+02
10% WS	3.54E+02	4.21E+02	7.41E+02

Table 14: Objective values of L2 level of SCI simulation, symmetric table with respect to the diagonal.

5.2 CASE 1: SS 90% - WS 10%

Since I am interested in the simulations with asymmetric muscle weakness, I will now analyze the case with the greatest asymmetry.

To simulate SCI in the most asymmetric case I reduced maximum isometric force of the muscles in the left leg (strong side = SS) to 90% and in the right leg (weak side = WS) to 10% of maximum isometric force.

Here are the results of joint angles, ground reaction force and muscle activations.

5.2.1 Joint angles

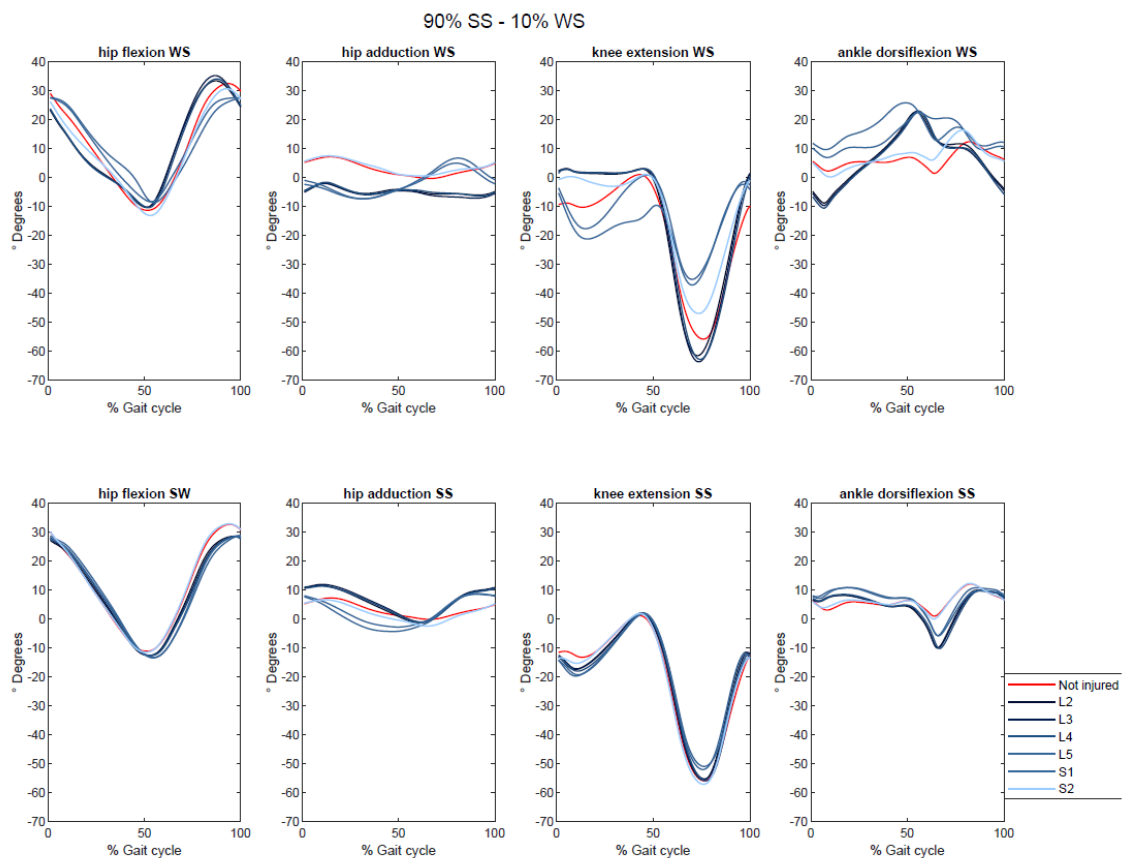


Fig. 8: joint angles of 7 SCI simulations, illustrating the variations in lower limb motion during different injury scenarios.

5.2.2 Ground reaction force

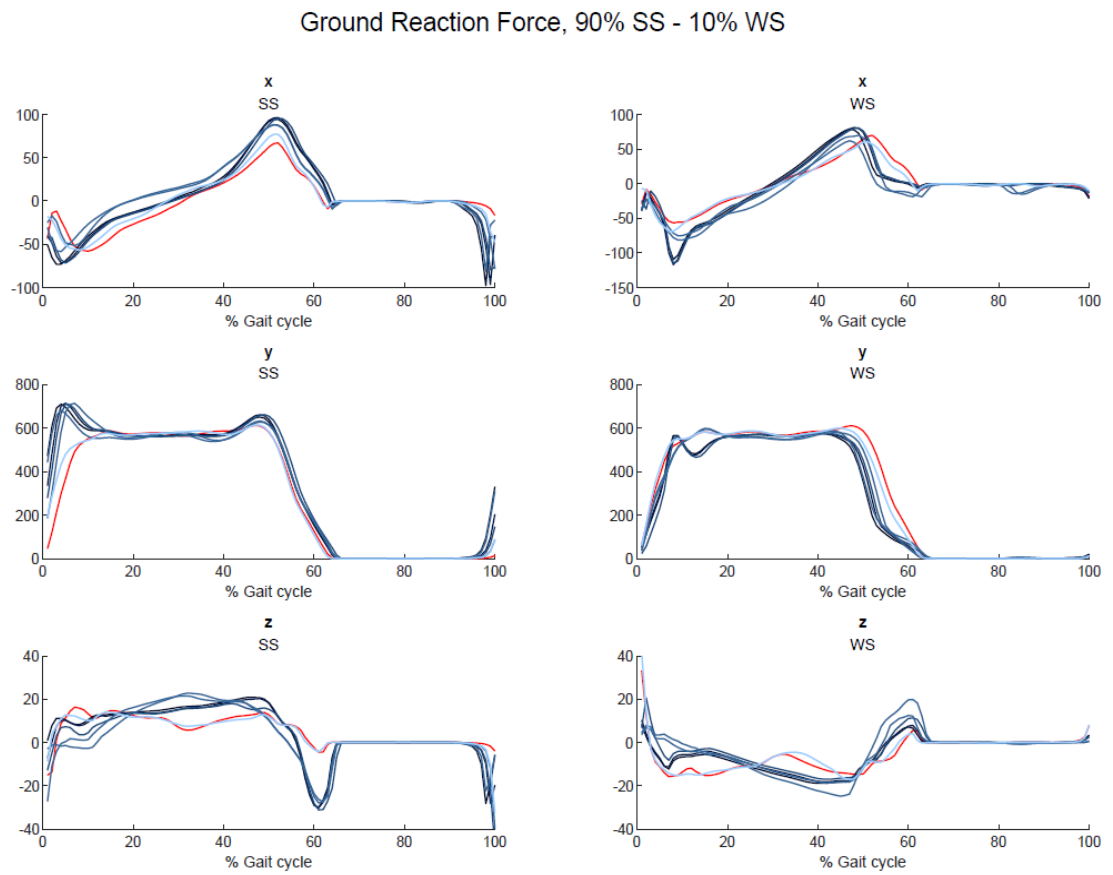


Fig. 9: *x, y, and z components of ground reaction force of strong (SS) and weak side (WS).*

5.2.3 Muscle activations

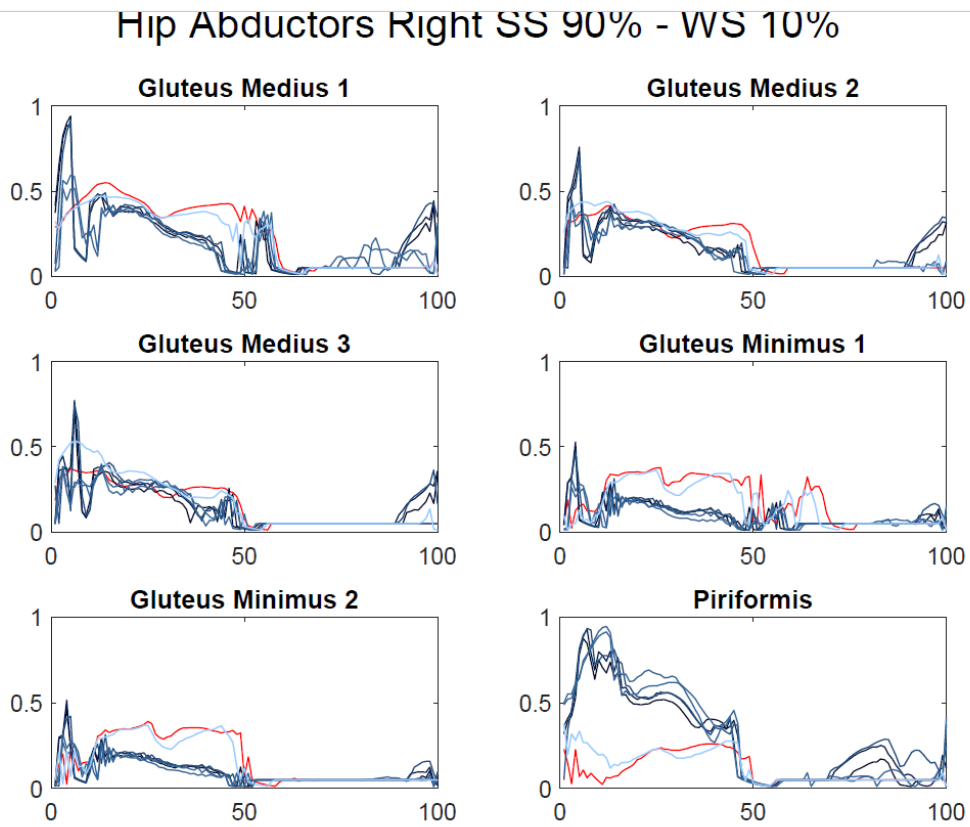


Fig. 10: Right hip abductor muscle activations in 90% - 10% SCI simulation.

Hip Abductors Left SS 90% - WS 10%

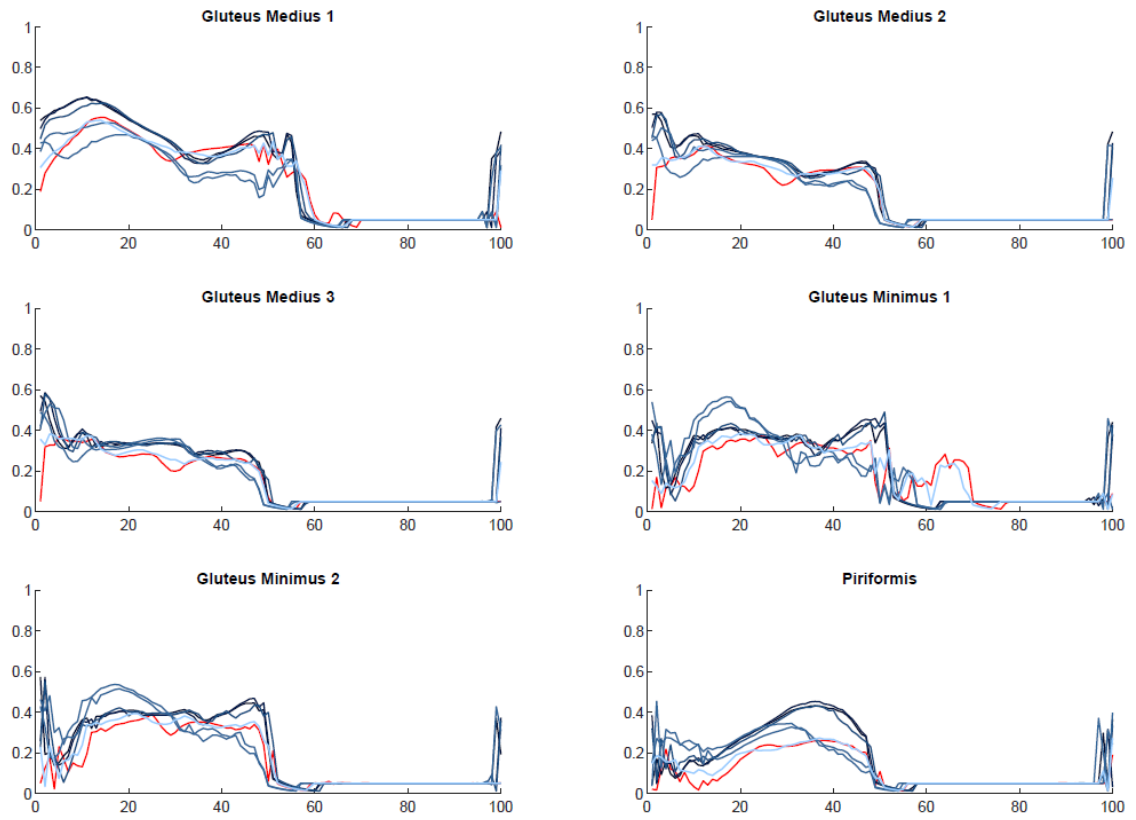


Fig. 11: Left hip abductor muscle activations in 90% - 10% SCI simulation.

Hip Extensors Right SS 90% - WS 10%

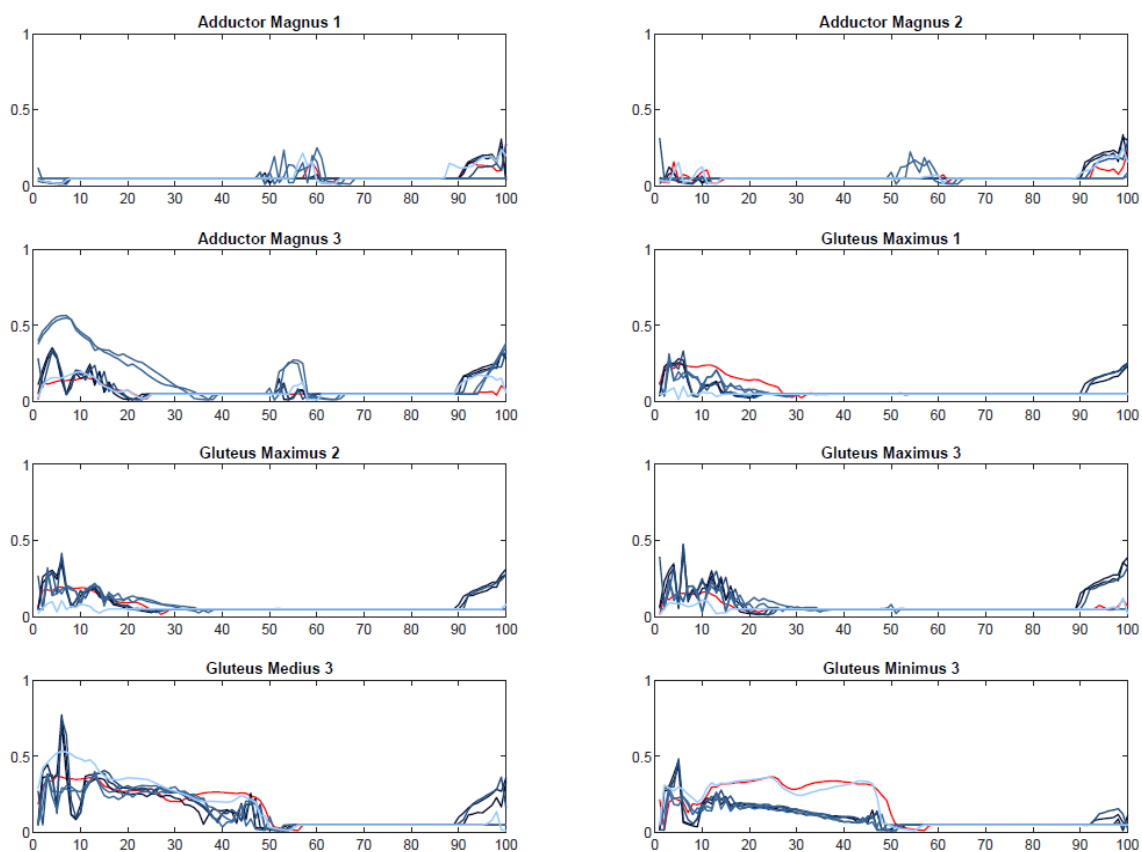


Fig. 12: Right hip extensor muscle activations in 90% - 10% SCI simulation.

Hip Extensors Left SS 90% - WS 10%

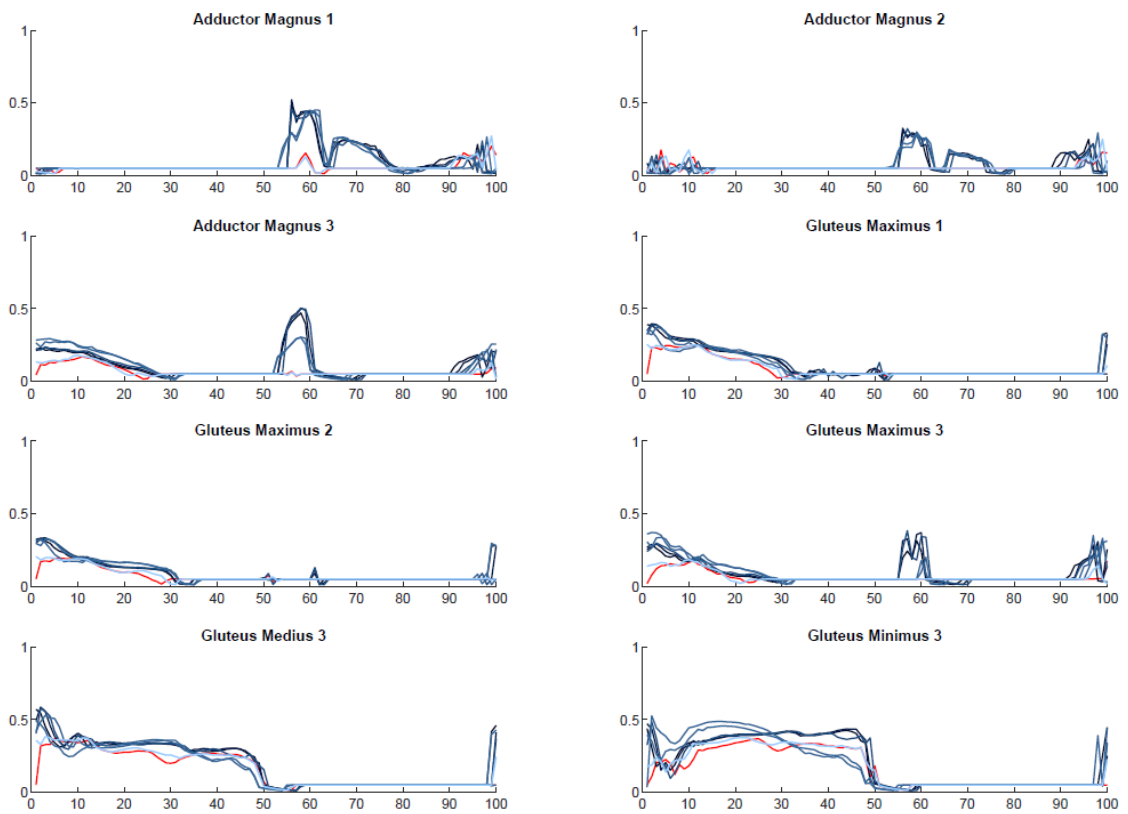


Fig. 13: Left hip extensor muscle activations in 90% - 10% SCI simulation.

Hip Flexors Right SS 90% - WS 10%

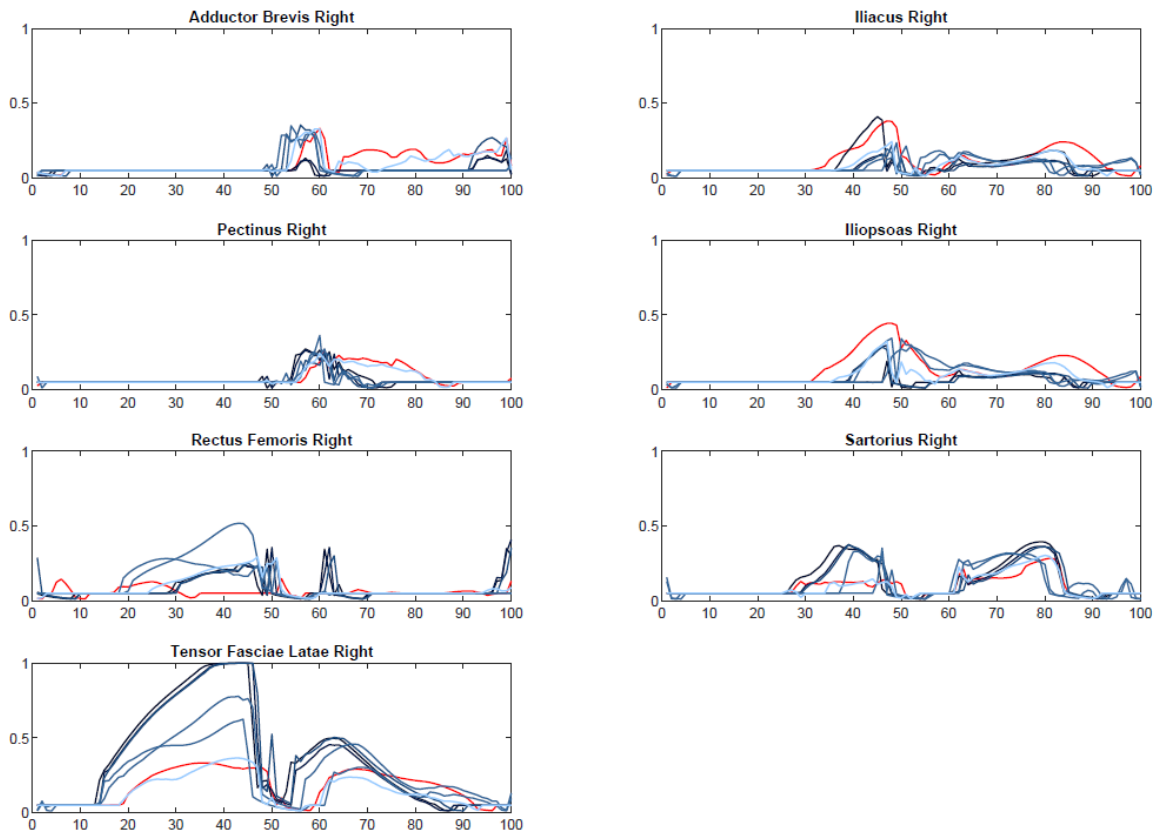


Fig. 14: Right hip flexor muscle activations in 90% - 10% SCI simulation.

Hip Flexors Left SS 90% - WS 10%

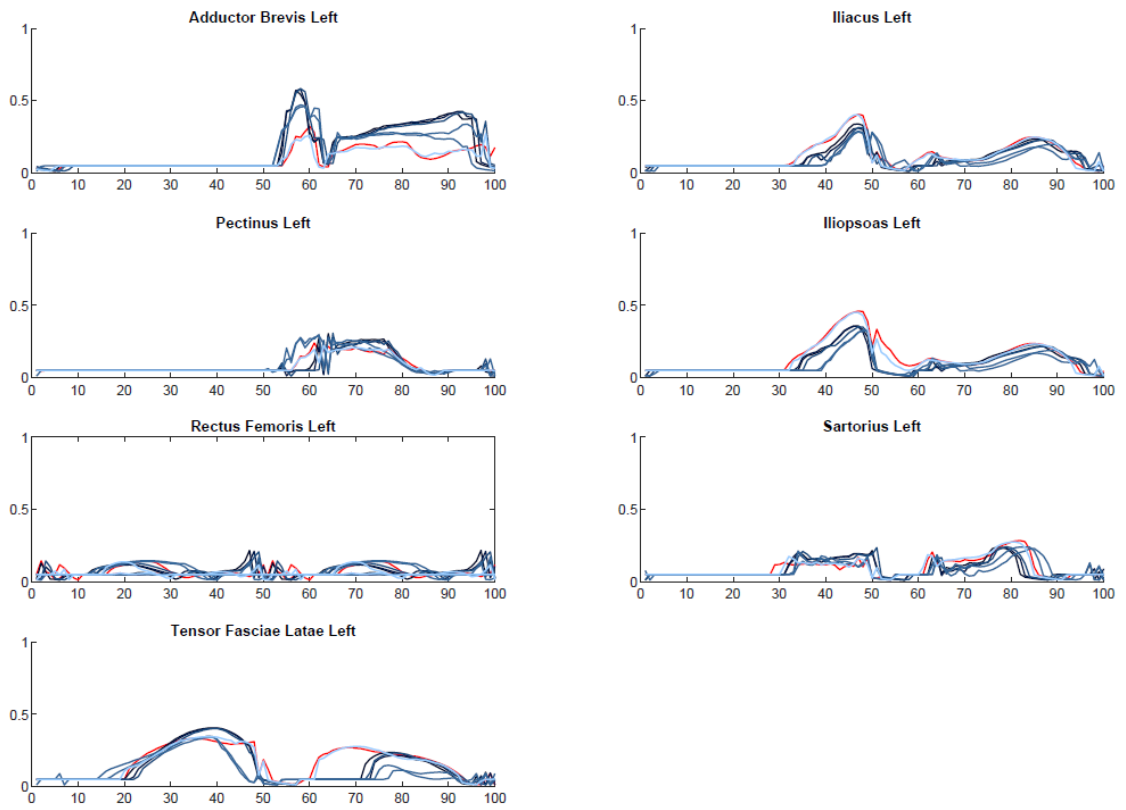


Fig. 15: Left hip flexor muscle activations in 90% - 10% SCI simulation.

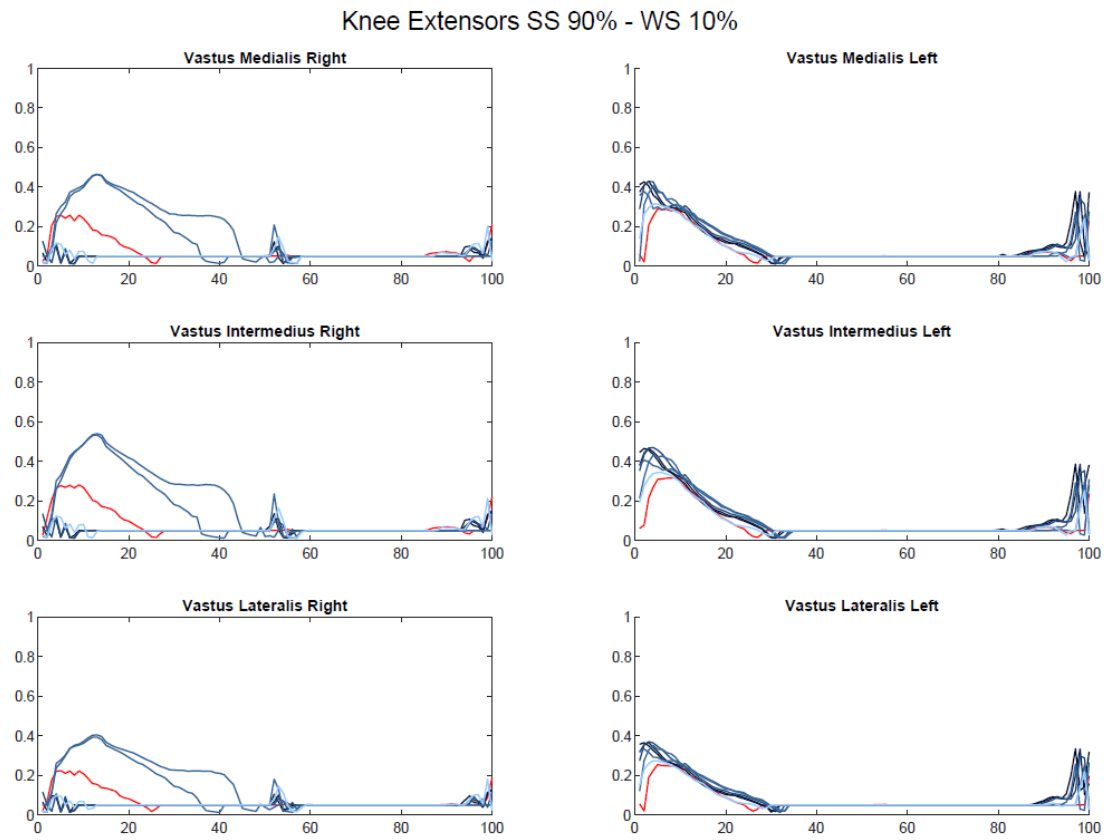


Fig. 16: Right and left knee extensor muscle activations in 90% - 10% SCI simulation.

Knee Flexors Right SS 90% - WS 10%

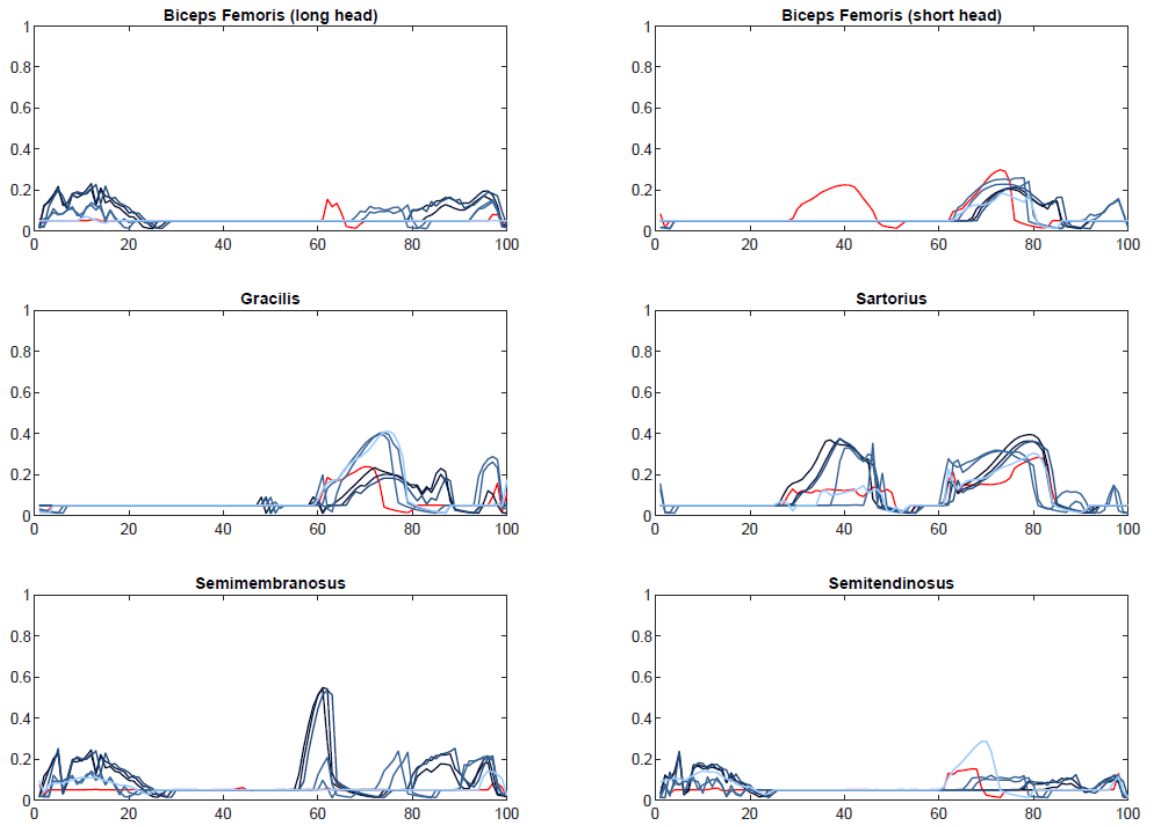


Fig. 17: Right knee flexor muscle activations in 90% - 10% SCI simulation.

Knee Flexors Left SS 90% - WS 10%

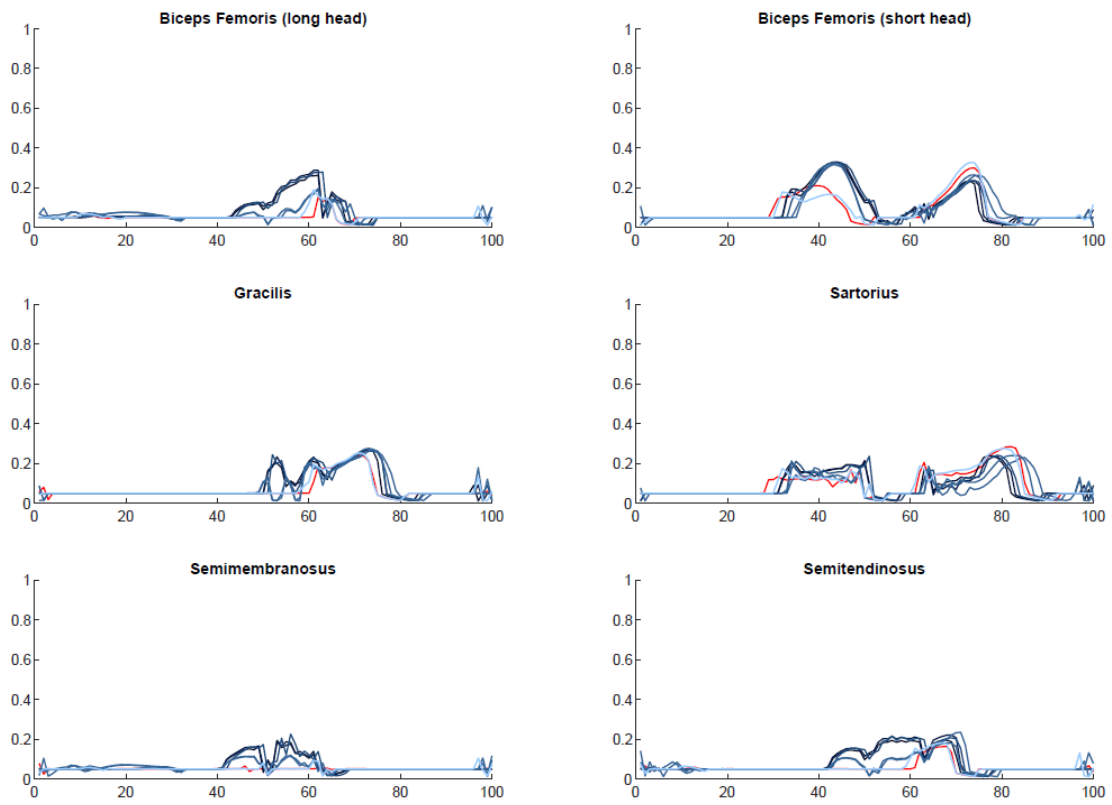


Fig. 18: Left knee flexor muscle activations in 90% - 10% SCI simulation.

Pantar Flexors Right SS 90% - WS 10%

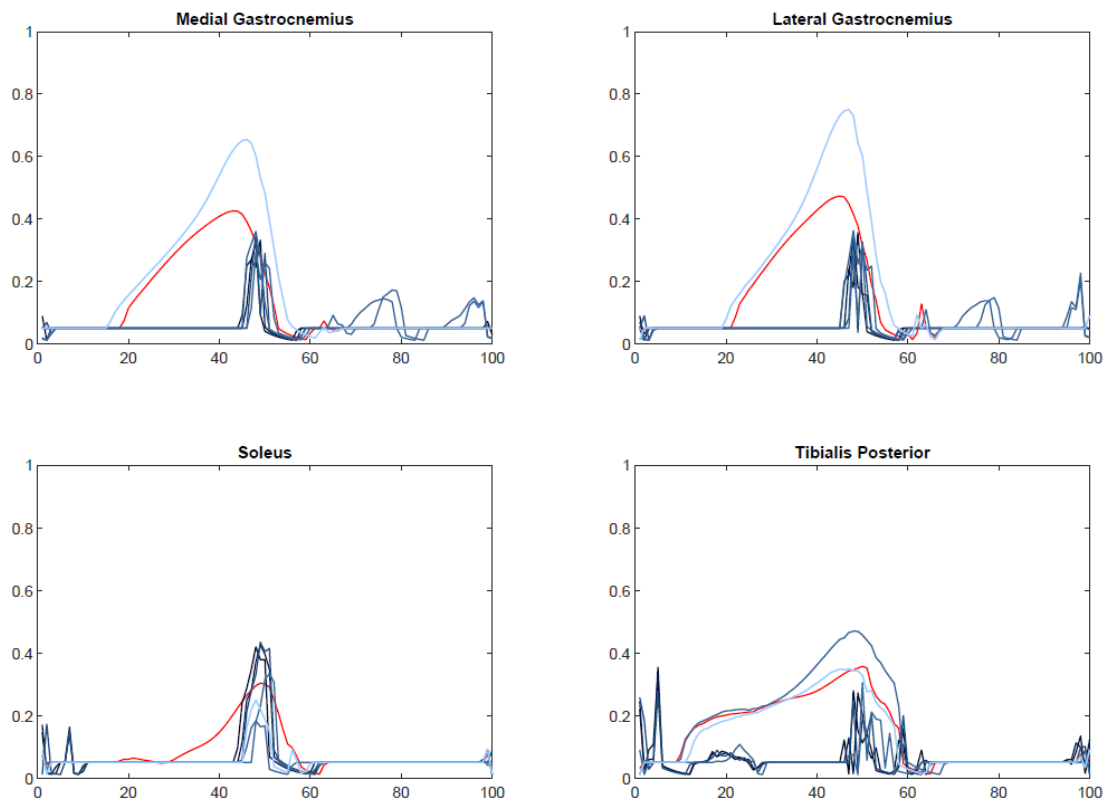


Fig. 19: Right plantar flexor muscle activations in 90% - 10% SCI simulation.

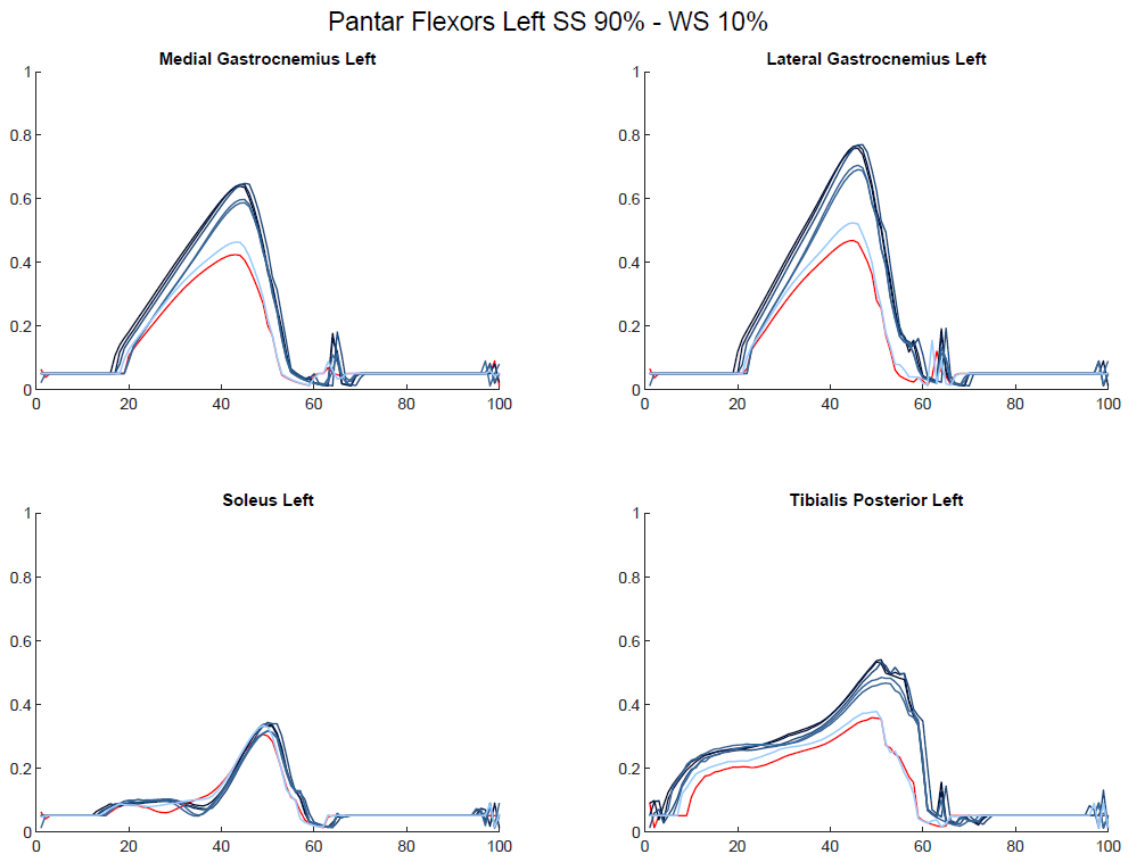


Fig. 20: Left plantar flexor muscle activations in 90% - 10% SCI simulation.

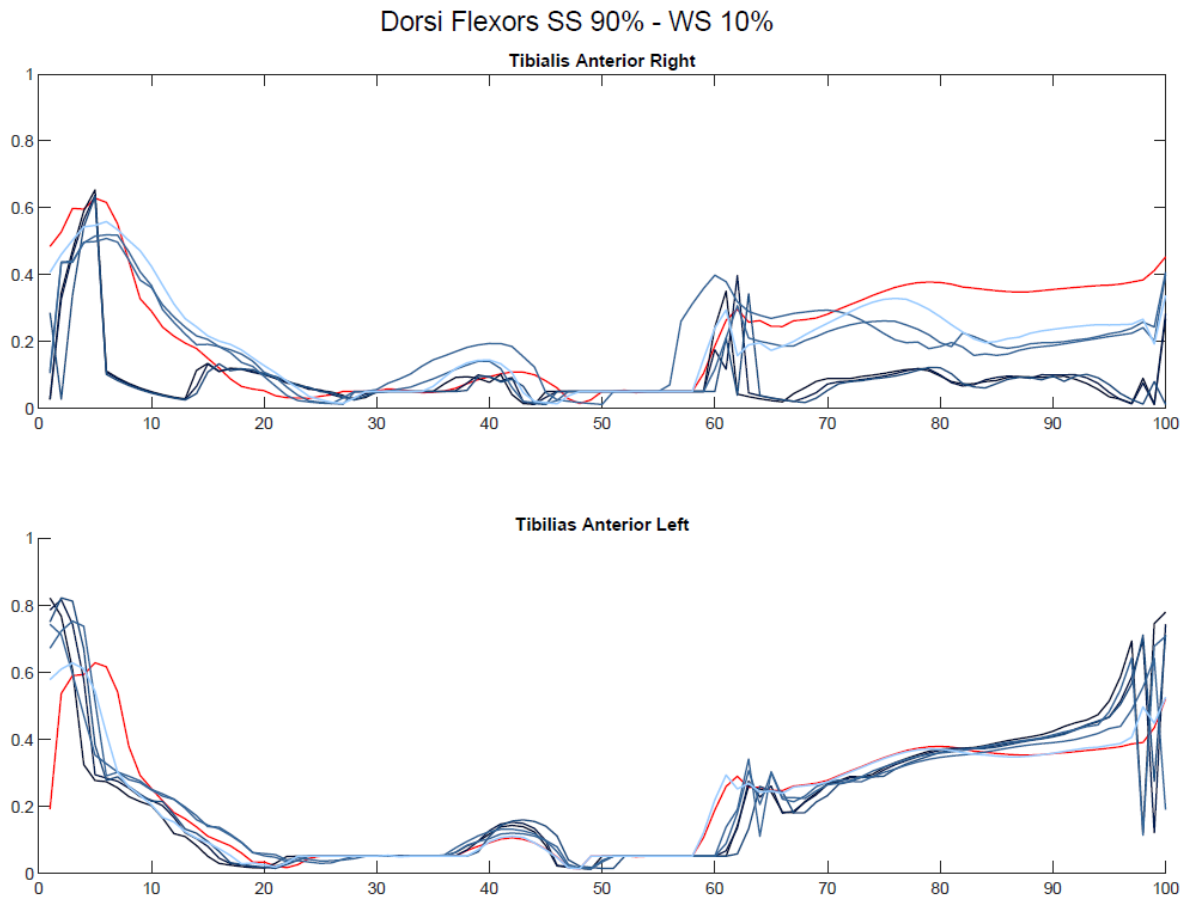


Fig. 21: Right and left dorsi flexor muscle activations in 90% - 10% SCI simulation.

5.3 CASE 2: SS 50% - WS 10%

To simulate SCI in the most severe case I reduced the muscles of the left leg (strong side = SS) to 50% of maximum isometric force and the muscles of the right leg (weak side = WS) to 10% of maximum isometric force.

Here are the results of joint angles, ground reaction force and muscle activations.

5.3.1 Joint angles

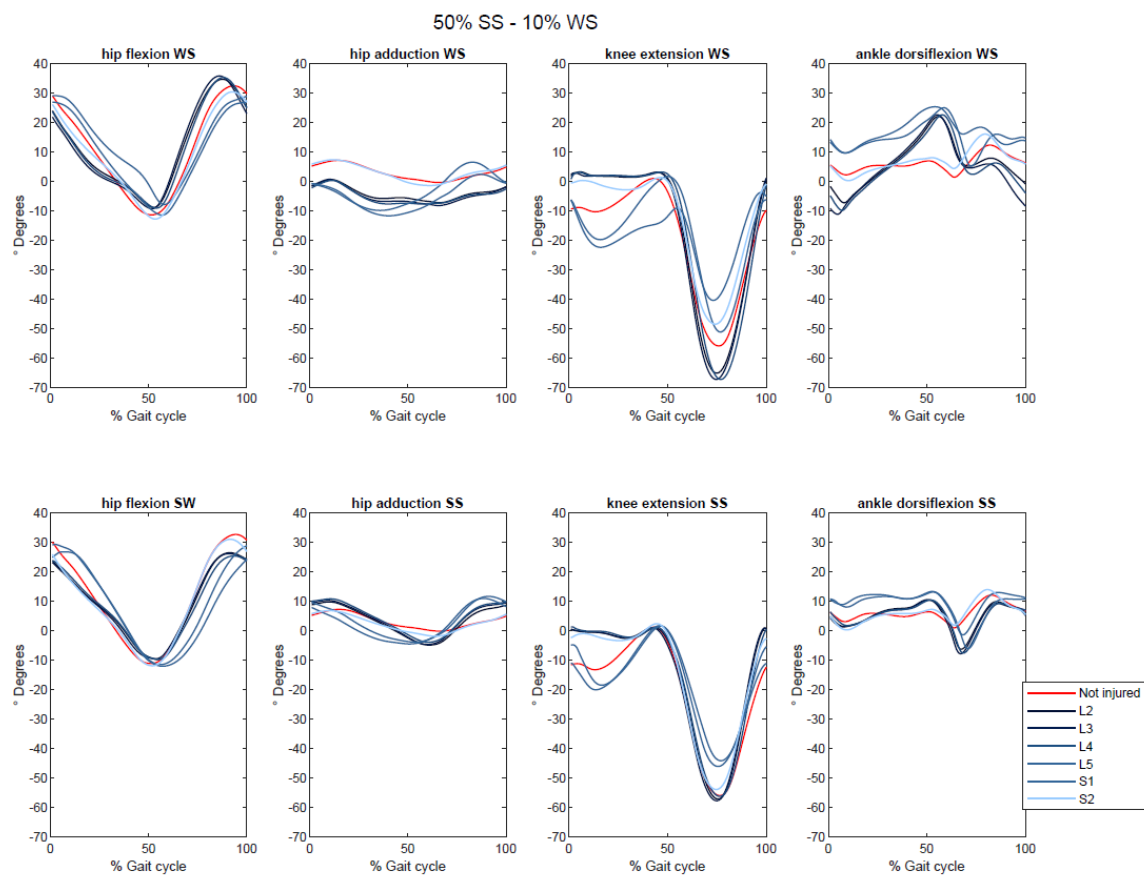


Fig. 22: joint angles of 7 SCI simulations, illustrating the variations in lower limb motion during different injury scenarios.

5.3.2 Ground reaction force

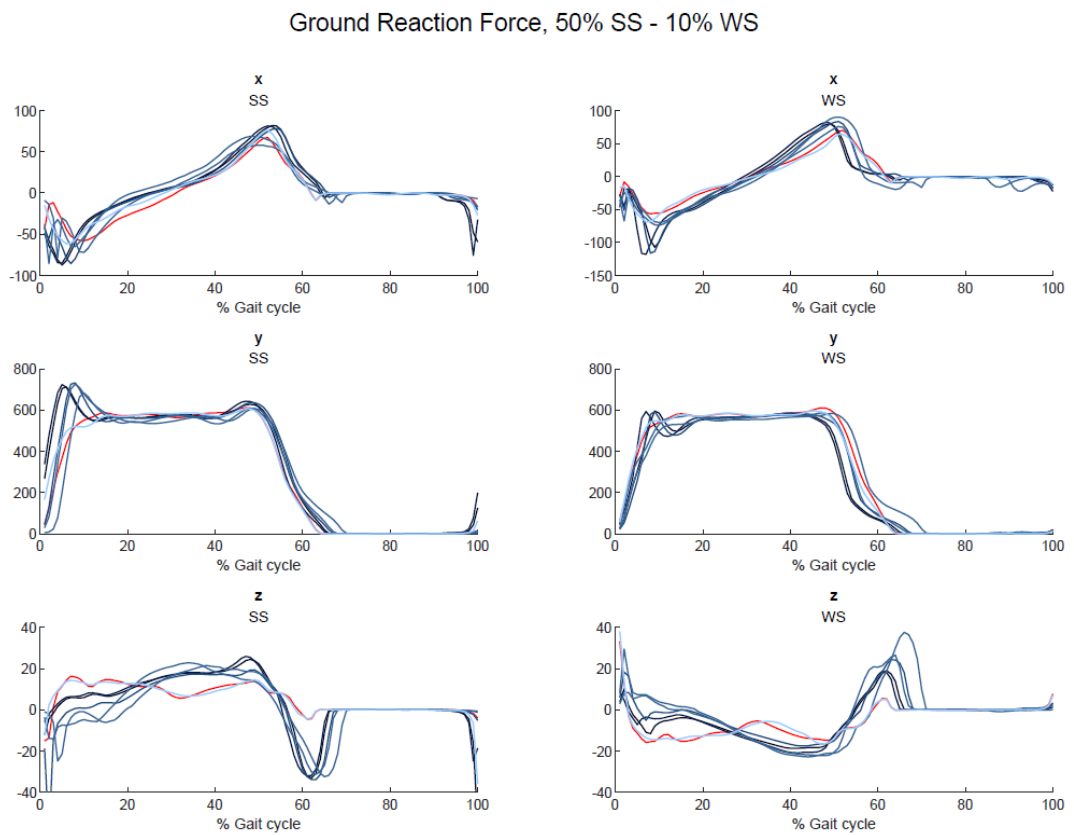


Fig. 23: x, y, and z components of ground reaction force of strong (SS) and weak side (WS).

5.3.3 Muscle activation

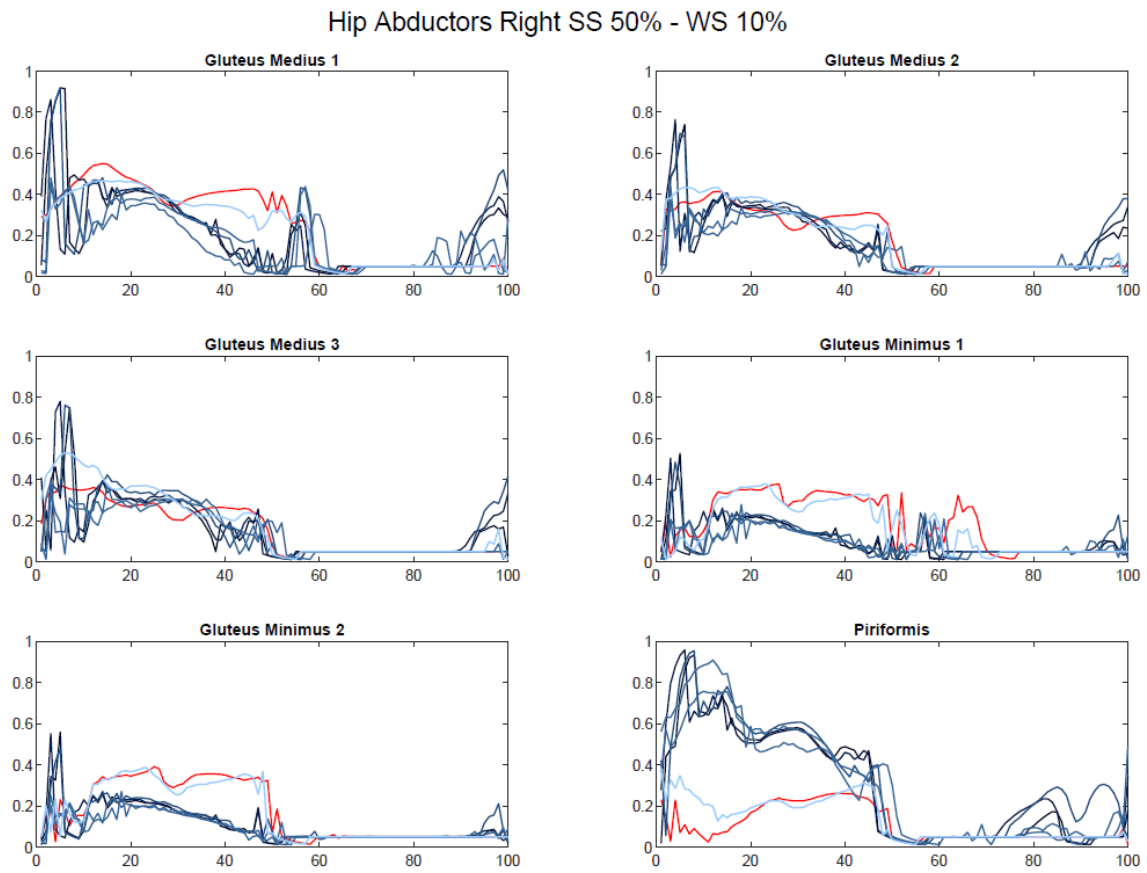


Fig. 24: Right hip abductor muscle activations in 50% - 10% SCI simulation.

Hip Abductors Left SS 50% - WS 10%

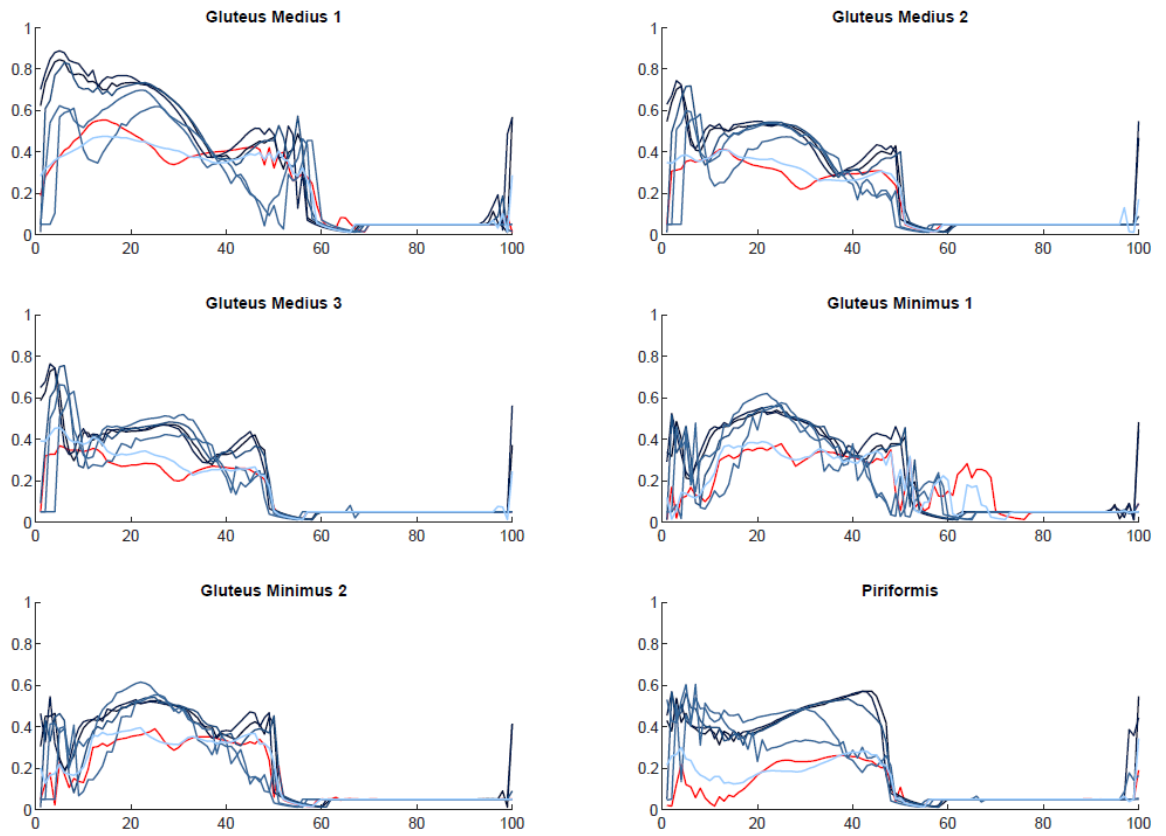


Fig. 25: Left hip abductor muscle activations in 50% - 10% SCI simulation.

Hip Extensors Right SS 50% - WS 10%

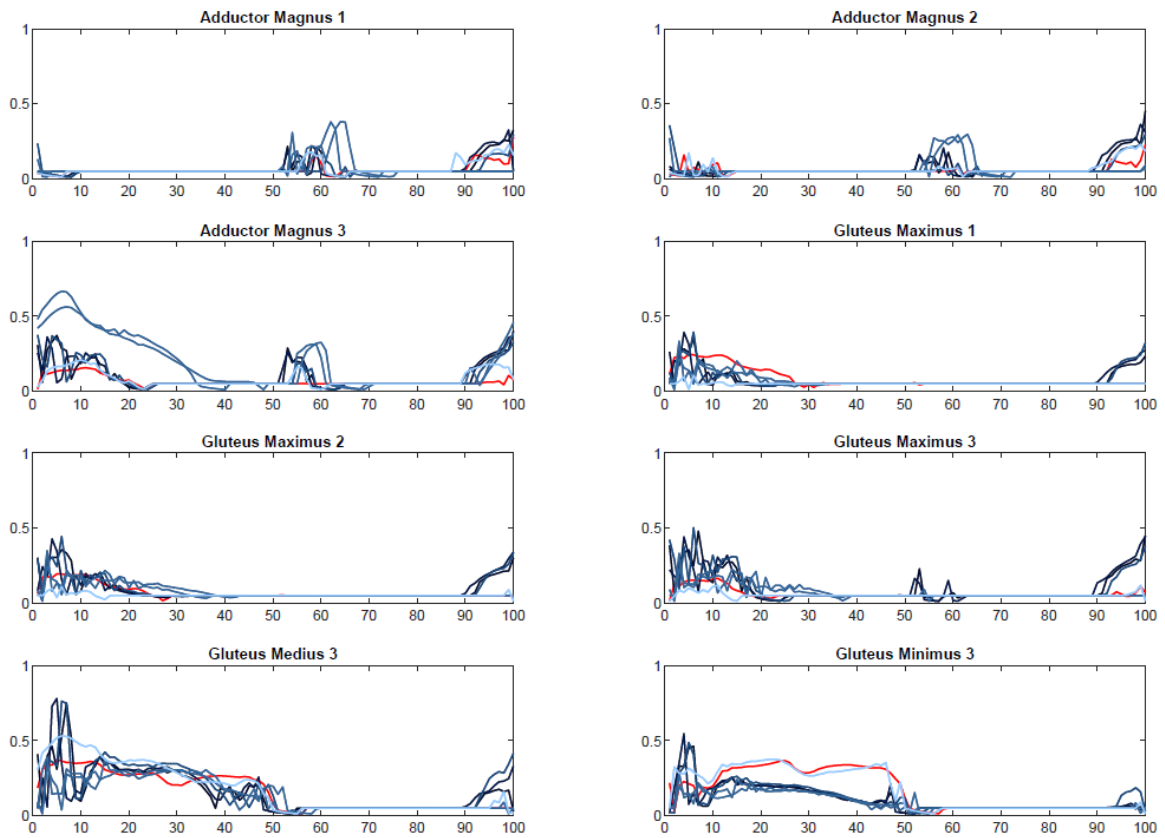


Fig. 26: Right hip extensor muscle activations in 50% - 10% SCI simulation.

Hip Flexors Right SS 50% - WS 10%

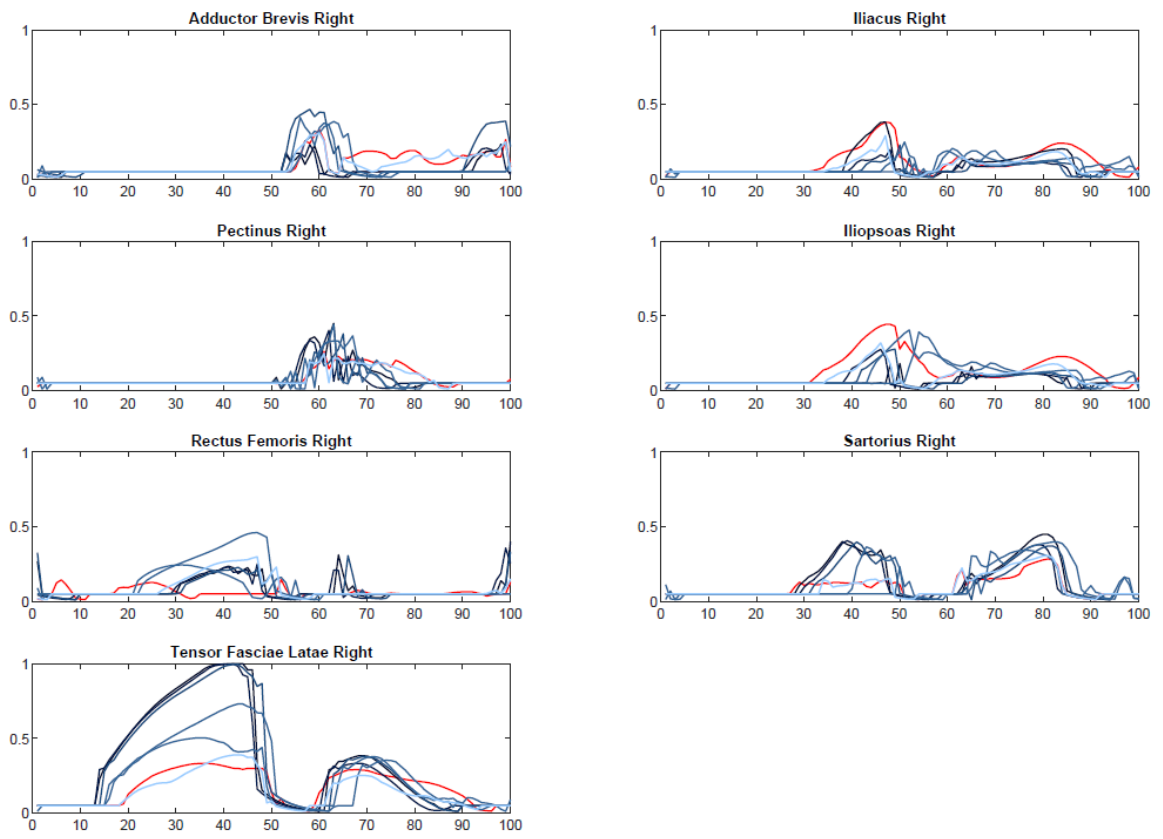


Fig. 27: Right hip flexor muscle activations in 50% - 10% SCI simulation.

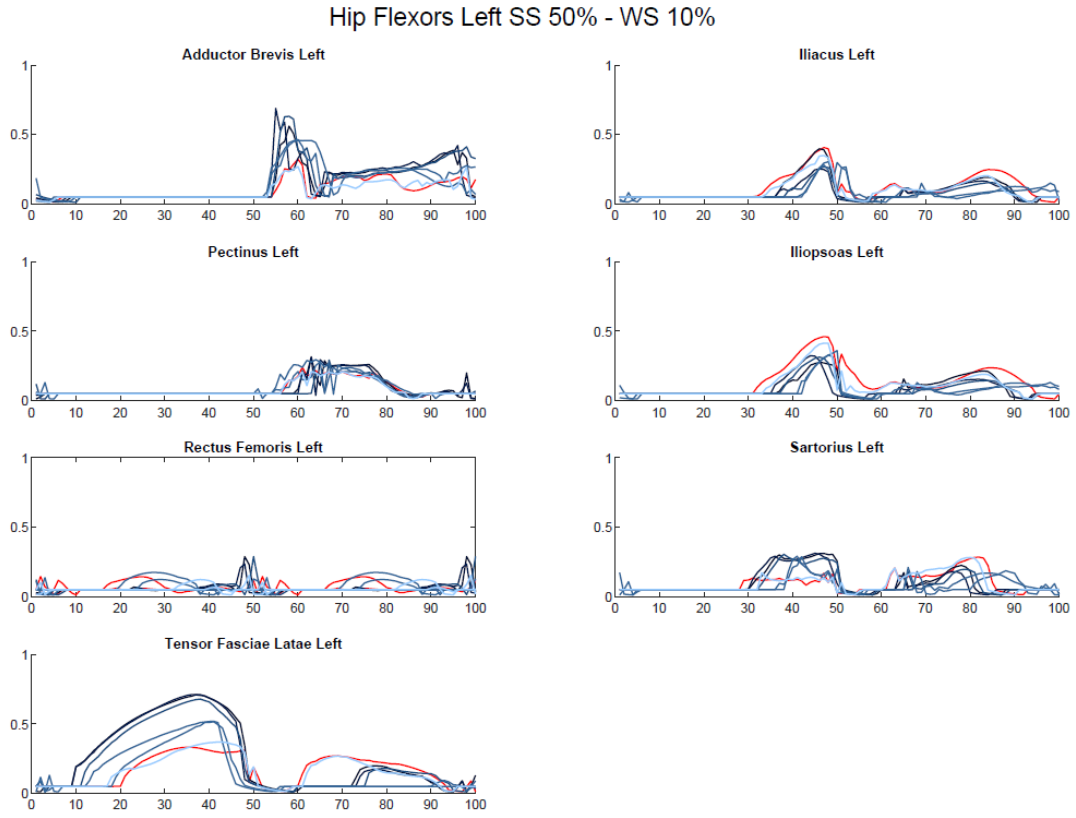


Fig. 28: Left hip flexor muscle activations in 50% - 10% SCI simulation.

Knee Extensors SS 50% - WS 10%

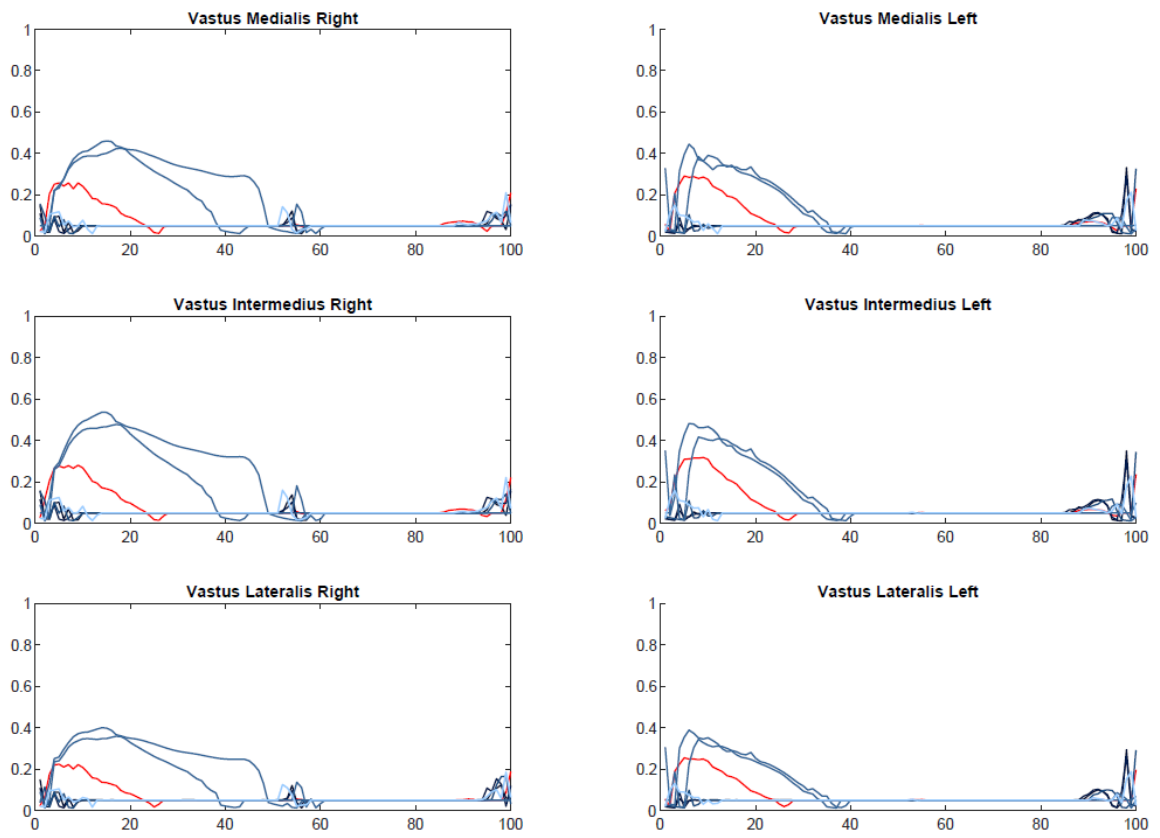


Fig. 29: Right and left knee extensor muscle activations in 50% - 10% SCI simulation.

Knee Flexors Right SS 50% - WS 10%

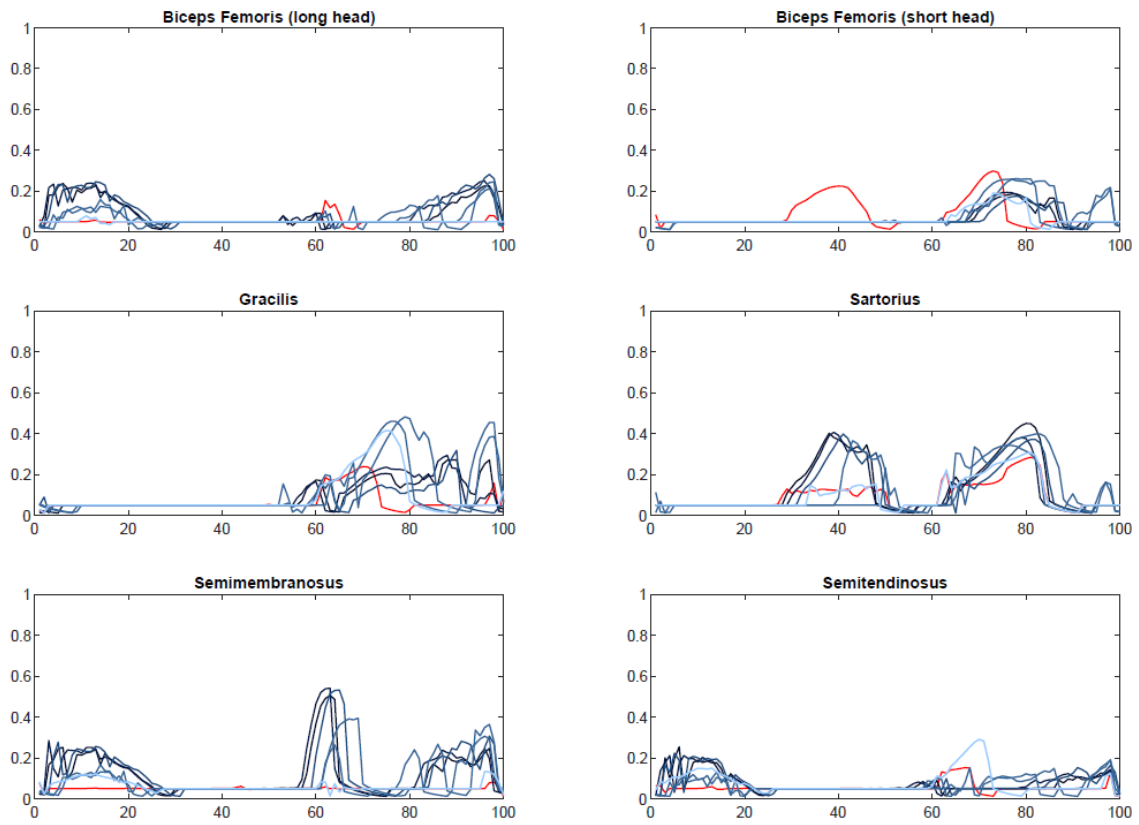


Fig. 30: Right knee flexor muscle activations in 50% - 10% SCI simulation.

Knee Flexors Left SS 50% - WS 10%

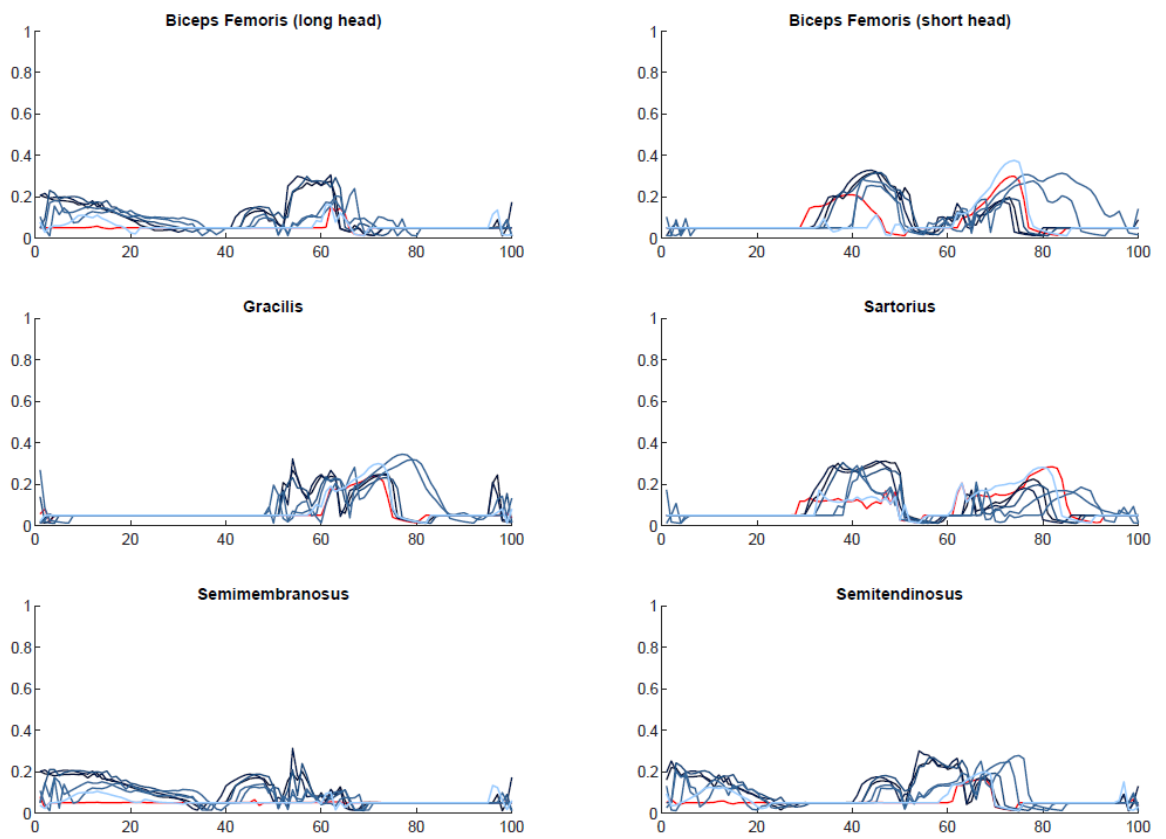


Fig. 31: Left knee flexor muscle activations in 50% - 10% SCI simulation.

Pantar Flexors Right SS 50% - WS 10%

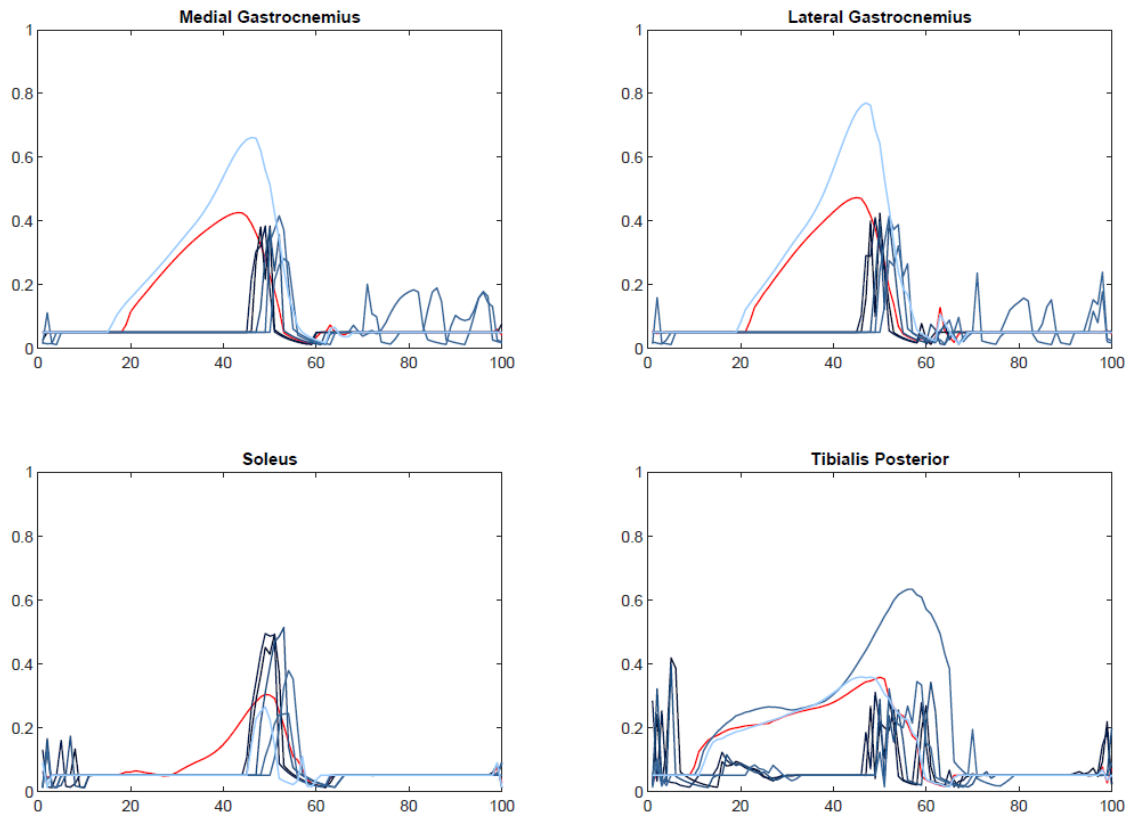


Fig. 32: Right plantar flexor muscle activations in 50% - 10% SCI simulation.

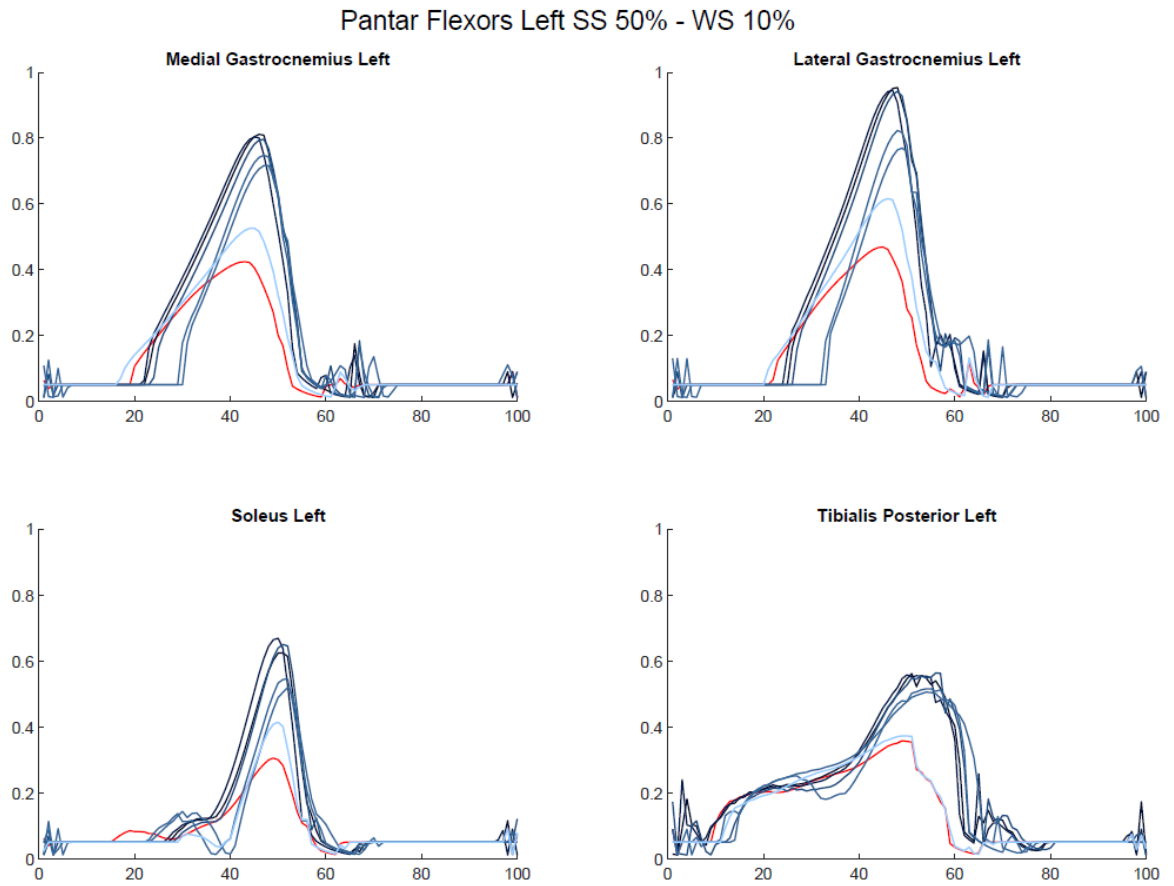


Fig. 33: Left plantar flexor muscle activations in 50% - 10% SCI simulation.

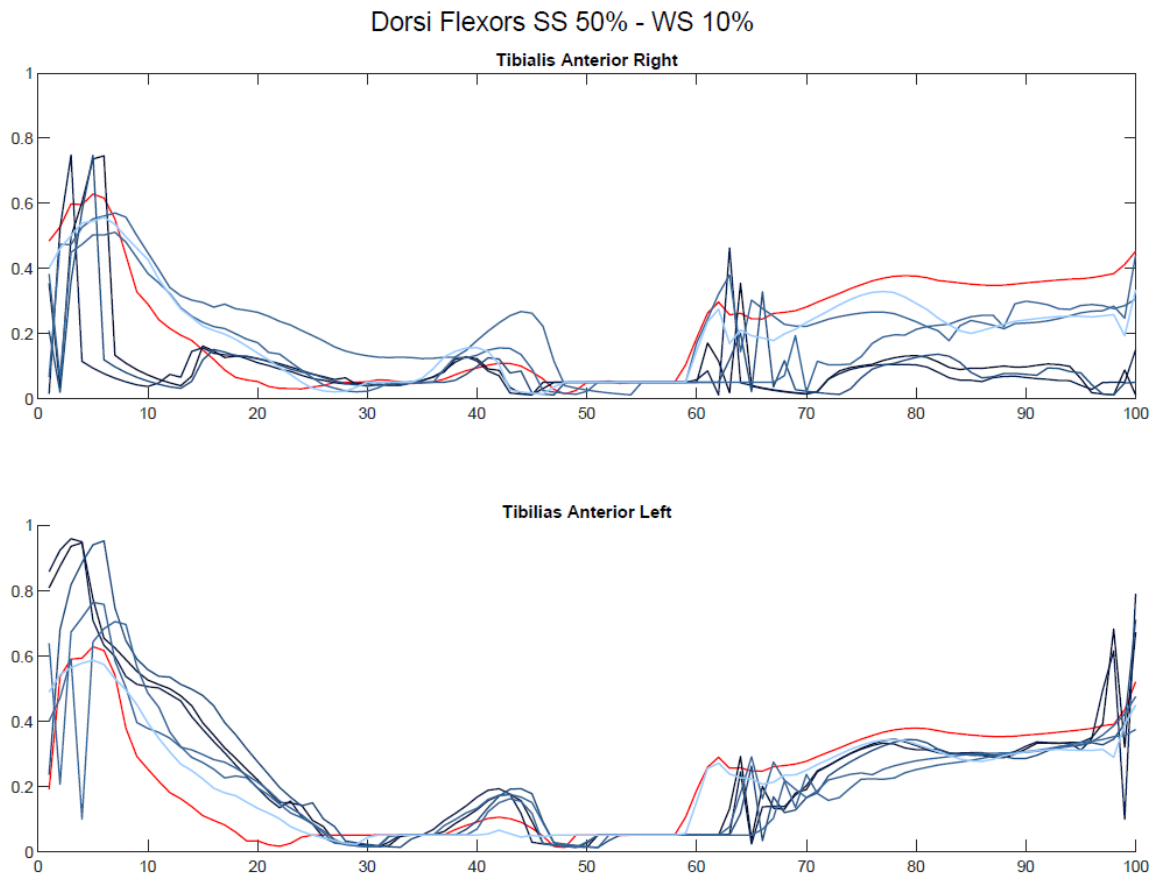


Fig. 34: Right and left dorsi flexor muscle activations in 50% - 10% SCI simulation.

Chapter 6 – Discussion of results

6.1 Objective value evaluation

Considering *Table 5*, that show the S2 SCI simulation results, two increasing trends are observed. Keeping the muscle weakness value of the weak leg constant and decreasing the muscle weakness value in the fixed leg, the objective value increases from $2.41E+02$ to $2.47E+02$, indicating a decrease in metabolic efficiency.

Similarly, the same trend is noted by keeping the muscle weakness value of the strong leg constant and decreasing the muscle weakness value of the weak leg.

As the severity of SCI increases, the difference between the objective values increases, reaching a difference of $3.87E+02$ vertically and $1.07E+02$ horizontally (*Table 14*) in the case of L2 SCI. This indicates a progressive decrease in metabolic efficiency.

More severe spinal cord injuries cause significant changes in the body's biomechanics. Deviations from normal posture and alterations in movement patterns are common in individuals with severe SCI. These changes increase the energetic cost of movements, as the body must adopt suboptimal strategies to maintain balance and functionality, thus contributing to the increase in the objective value in the simulations.

The performance of the model with 90% functionality post-spinal cord injury shows a slight decrease in the objective function ($2.41E+02$) compared to the model without injuries ($2.43E+02$). This is because the uninjured model is constrained to walk at a fixed speed of 0.8 m/s, which is slower than the average walking speed of a healthy individual. As a result, the uninjured model requires more energy to maintain a slower pace, putting a greater demand on its system.

Conversely, despite simulating a spinal cord injury, the model with 90% functionality may require less effort and energy consumption than the uninjured model, leading to a lower overall goal value. It should be noted that the difference in objective values between the two models is relatively small.

It is essential to consider these factors when analyzing the performance and energy consumption of the models in this study.

6.2 Gait phases duration

Since the velocity is fixed, the model distributes the subphases differently during the gait cycle, varying levels of muscle weakness.

Based on the results presented in Chapter 6, it is evident that an increase in SCI severity and asymmetry between the strong and weak legs significantly reduces the percentage of single support.

Overall, in the most severe SCI case, the entire stance phase lasts longer than in the other simulations. This extended stance phase in severe SCI cases can be attributed to the increased instability and compromised motor control, requiring more time to ensure balance and support during walking. The body compensates for the weakened leg by prolonging the stance phase, which provides additional stability but reduces overall gait efficiency. This is particularly evident in L5 (Table 9), L4 (Table 11), L3 (Table 13) and L2 (Table 15) where the stance phase exceeds 70% of the gait cycle, compared to 65% in normal walking.

6.3 CASE 1: SS 90% - WS 10%

Analyzing joint angle, ground reaction force and muscle activation plots, it is clearly possible to classify the simulation I did (from L2 to S2) in three groups, based on the trend of the plots.

GROUP 1: S2 SCI simulation

GROUP 2: L5 and S1 SCI simulations

GROUP 3: L4, L3 and L2 SCI simulations

Joint angle (Fig. 8)

During the simulation of group 1, it was observed that despite muscle weakness, the model was able to compensate and exhibited nearly normal gait patterns. The plots depicting overall joint angle followed the patterns observed in the simulation of individuals without injury.

The simulations from group 2 indicate increased dorsiflexion throughout the entire gait cycle. This is attributed to weaker plantar flexors (Fig. 19), particularly during the stance phase, which also impacts the knee joint. As a result, the knee exhibits greater flexion but with a reduced range of motion compared to the 'not injured' condition.

In group 3, simulation demonstrates a plantarflexion that exceeds that of the 'not injured' group in the weak side simulation. Additionally, there is limited knee flexion in the first half of the gait cycle, followed by increased knee flexion compared to the 'not injured' group. The weak hip is consistently abducted throughout the entire gait cycle.

Ground reaction force (Fig. 9)

X Component (Anterior-Posterior Forces):

In simulations where a leg is stronger than the other one, it was observed that the second peak increased for each level of spinal cord injury compared to individuals without injuries. An unusually high positive peak in the x-component suggests a more forceful propulsion during the push-off phase of the gait cycle, when the foot lifts off the ground to propel the body forward. The left gastrocnemius and tibialis posterior muscles show increased activation during this phase (Fig. 20).

Towards the end of the gait cycle, the x-component of the Ground Reaction Force demonstrates a trend towards highly negative values, indicating a significant braking force. This occurs when the foot is in the pre-contact or initial contact phase with the ground, as the body prepares to absorb impact and stabilize weight for the next step. The left tibialis anterior muscle shows increased activity during this phase (Fig. 21).

In simulation with a weakened leg due to spinal cord injury, there is a noticeable increase in severity indicated by the first negative peak being more pronounced than observed in individuals without injury. This suggests a greater impact force upon landing, requiring a heightened braking action to decelerate and stabilize the body. The gluteus medius and minimus muscles show increased activation during this phase (Fig. 6). Additionally, as the severity of the spinal cord injury worsens, there is an advancement of the positive peak. An early positive peak in the x-component of the Ground Reaction Force indicates an earlier propulsion force in the gait cycle. The soleus muscle is more engaged during this phase (Fig. 19).

Y Component (Vertical Forces):

On the strong side, the initial peak is elevated for groups 2 and 3, indicating a heightened initial force of the strong foot contacting the ground. This is associated with a compensatory strategy adopted in the presence of significant weakness in the other leg. This results in a harder and more forceful landing on the strong leg, as the body seeks to rapidly stabilize the weight on a support base perceived as more secure.

On the weaker side, the second peak in force is lower, suggesting a decrease in push-off force during the toe-off phase when the foot is lifted from the ground. Specifically, in this phase, the activation of the plantar flexors (Fig. 19) on the affected side is lower compared to the non-injured side.

6.4 CASE 2: SS 50% - WS 10%

Joint angle (Fig. 22)

In the simulation of group 1, it was observed that the overall pattern aligns with the 'Not injured' trend, except for knee extension. Indeed, both knees exhibit stiffness with a notably reduced range of motion, especially during the initial stages of the gait cycle. During the first double support phase, knee extensors in the stronger legs show lesser activation (Fig. 29).

The simulations of group 2 indicate increased abduction on both sides during the first half of the gait cycle. The piriformis on the weaker side exhibits higher activation compared to the 'not injured' level (Fig. 24), and the abductors on the stronger side generally show higher activation than the 'Not injured' level during this phase (Fig. 25). Both knees demonstrate increased flexion during the first half of the gait cycle, and both ankles exhibit greater dorsiflexion than the 'Not injured' level. Dorsiflexors on the weaker side are more activated (Fig. 34).

In group 3, evidence suggests that on the weak side, the model is abducting the hip throughout the entire gait cycle (Fig. 6.16), while on the strong side, adduction is accentuated, as indicated by increased muscle activation (Fig. 25).

Ground reaction force (Fig. 23)

In simulations of SCI in case 2, the peaks of the x and y components of the ground reaction force are more pronounced. This occurs because the weakened muscles are less able to

control and stabilize the body during movement, leading to more significant shifts in force as the body compensates. The increased peaks in the x-component suggest a more forceful and possibly less controlled propulsion during the push-off phase, while the heightened peaks in the y-component indicate greater vertical forces as the body struggles to maintain balance and stability.

The various simulations can still be classified into three groups.

Chapter 7 – Conclusions and limitations of the study

In this chapter, I explore the conclusions and limitations of my study.

It is essential to identify and acknowledge the constraints that may have influenced my findings and evaluate how these limitations affect the generalizability and reliability of my results.

7.1 Conclusions

In both analyzed cases (90%-10% and 50%-10%) and the other ones not analyzed, it is possible to classify the simulation into three distinct groups. This classification allows for a clearer analysis and understanding of the simulation results, providing a structured framework to interpret the variations and outcomes observed under these different scenarios. By categorizing the data in this manner, I could more effectively compare and contrast the impacts of each case, thereby enhancing the overall insights derived from the study.

The S2 SCI level is like the 'Not injured' case, as I anticipated, and this is confirmed by objective values (Table 5).

The data clearly indicate that the S2 level remains nearly consistent with the baseline measurements of the 'Not injured' scenario, reinforcing the reliability of my initial expectations. The objective values presented offer evidence in support of the conclusion that the S2 SCI level shows minimal deviation, thus confirming the hypothesis and enhancing the overall validity of the study.

The analysis reveals that an increase in objective values corresponds to an increase in muscle weakness. This relationship is evident across the data, where higher objective measurements consistently align with greater degrees of muscle impairment. This finding highlights the significance of monitoring these objective values as accurate indicators of muscle strength. By recognizing this relationship, it is possible to evaluate the degree of muscle weakness and customize interventions to address the unique needs of individuals experiencing muscle deterioration.

7.2 Limitations

Upon analyzing the model, it is apparent that there are identifiable limitations, particularly regarding the portrayal of plantar flexion of the foot. Plantar flexion, an essential element of human movement, involves the downward motion of the foot, predominantly due to the contraction of the calf muscles and the extension of the ankle joint. However, the model may not accurately capture the complexities and nuances of this movement, resulting in differences between simulated results and actual observations in healthy individuals.

An additional limitation is that the weights of the cost function were not adjusted during the various simulations. It is important to acknowledge that the severity of injuries may differ, which could potentially impact the importance of different cost components within the function. While initially assigning equal weights to each level of injury, adjustments may be needed to accurately reflect the varying degrees of severity. By dynamically adapting these weights based on the characteristics of each injury level, the objective function can effectively capture the complexities of injury assessment. This, in turn, can help inform decision-making in injury management and prevention strategies.

In the experimental setup, the model was forced to walk at a constant speed throughout the simulations. This decision was made to ensure consistency across trials and allow for direct comparisons of results. However, it is important to recognize that the fixed speed may not accurately represent the various walking speeds observed in real-world situations. For some simulations the set speed is too fast, potentially leading to differences in biomechanics or unrealistic walking patterns. On the other hand, other simulations may find the speed too slow, which could also impact the accuracy of the simulated movements. Therefore, while the standardized speed helps control experimental variables, its limitations underscore the importance of future research to incorporate more dynamic and adaptable locomotion parameters that better reflect the natural variability of human walking behavior.

Bibliography

1. Pirker, Walter & Katzenschlager, Regina. (2016). Gait disorders in adults and the elderly: A clinical guide. *Wiener klinische Wochenschrift*. 129. 10.1007/s00508-016-1096-4.
2. Winter, D. A. (1991). *Biomechanics and motor control of human gait: normal, elderly and pathological*.
3. (2010). Gait Analysis: Normal and Pathological Function. *Journal of Sports Science & Medicine*, 9(2), 353.
4. Kim, J. I., Imaizumi, K., Thete, M. V., Hudacova, Z., Jurjuț, O., Amin, N. D., Scherrer, G., & Pașca, S. P. (2024). Human assembloid model of the ascending neural sensory pathway. *bioRxiv: the preprint server for biology*, 2024.03.11.584539.
5. Lemon R. N. (2008). Descending pathways in motor control. *Annual review of neuroscience*, 31, 195–218.
6. Rupp, R., Biering-Sørensen, F., Burns, S. P., Graves, D. E., Guest, J., Jones, L., Read, M. S., Rodriguez, G. M., Schuld, C., Tansey-Md, K. E., Walden, K., & Kirshblum, S. (2021). *International Standards for Neurological Classification of Spinal Cord Injury: Revised 2019*.
7. Kirshblum, S. C., Burns, S. P., Biering-Sorensen, F., Donovan, W., Graves, D. E., Jha, A., Waring, W. (2011). *International standards for neurological classification of spinal cord injury (Revised 2011)*. *The Journal of Spinal Cord Medicine*, 34(6), 535–546.
8. Bican, O., Minagar, A., & Pruitt, A. A. (2013). The spinal cord: a review of functional neuroanatomy. *Neurologic clinics*, 31(1), 1–18.
9. Cicirelli, G., Impedovo, D., Dentamaro, V., Marani, R., Pirlo, G., & D'Orazio, T. R. (2022). Human Gait Analysis in Neurodegenerative Diseases: A Review. *IEEE journal of biomedical and health informatics*, 26(1), 229–242.
10. Aggarwal, J. K., & Cai, Q. (1999). Human motion analysis: A review. *Computer vision and image understanding*, 73(3), 428-440.
11. Dietz, V., & Müller, R. (2004). Degradation of neuronal function following a spinal cord injury: mechanisms and countermeasures. *Brain*, 127(10), 2221-2231.

12. Boulenguez, P., Liabeuf, S., Bos, R., Bras, H., Jean-Xavier, C., Brocard, C., ... & Vinay, L. (2010). Down-regulation of the potassium-chloride cotransporter KCC2 contributes to spasticity after spinal cord injury. *Nature medicine*, 16(3), 302-307.
13. Sharrard, W. J. W. (1964). The segmental innervation of the lower limb muscles in man: Arris and Gale lecture delivered at the Royal College of Surgeons of England on 2nd January 1964. *Annals of the Royal College of Surgeons of England*, 35(2), 106.
14. Ditunno, P. L., Patrick, M., Stineman, M., & Ditunno, J. F. (2008). Who wants to walk? Preferences for recovery after SCI: a longitudinal and cross-sectional study. *Spinal cord*, 46(7), 500–506.
15. Delp, S. L., Anderson, F. C., Arnold, A. S., Loan, P., Habib, A., John, C. T., Guendelman, E., & Thelen, D. G. (2007). OpenSim: open-source software to create and analyze dynamic simulations of movement. *IEEE transactions on biomedical engineering*, 54(11), 1940–1950.
16. Seth, A., Hicks, J. L., Uchida, T. K., Habib, A., Dembia, C. L., Dunne, J. J., ... & Delp, S. L. (2018). OpenSim: Simulating musculoskeletal dynamics and neuromuscular control to study human and animal movement. *PLoS computational biology*, 14(7), e1006223.
17. Thelen, D. G., & Anderson, F. C. (2006). Using computed muscle control to generate forward dynamic simulations of human walking from experimental data. *Journal of biomechanics*, 39(6), 1107–1115.
18. Deb, Kalyan. (2001). *Multiobjective Optimization Using Evolutionary Algorithms*. Wiley, New York.
19. Roelker, S. A., Caruthers, E. J., Baker, R. K., Pelz, N. C., Chaudhari, A. M. W., & Siston, R. A. (2017). Interpreting Musculoskeletal Models and Dynamic Simulations: Causes and Effects of Differences Between Models. *Annals of Biomedical Engineering*, 45(11), 2635-2647.
20. Falisse, A., Afschrift, M., & De Groote, F. (2022). Modeling toes contributes to realistic stance knee mechanics in three-dimensional predictive simulations of walking. *PloS one*, 17(1), e0256311.
21. Falisse, A., Serrancolí, G., Dembia, C. L., Gillis, J., Jonkers, I., & De Groote, F. (2019). Rapid predictive simulations with complex musculoskeletal models suggest that diverse healthy and pathological human gaits can emerge from similar control strategies. *Journal of the Royal Society, Interface*, 16(157), 20190402.

22. Bhargava, L. J., Pandy, M. G., & Anderson, F. C. (2004). A phenomenological model for estimating metabolic energy consumption in muscle contraction. *Journal of biomechanics*, 37(1), 81-88.
23. Jamison, Steve & Pan, Xueliang & Chaudhari, Ajit. (2012). Knee moments during run-to-cut maneuvers are associated with lateral trunk positioning. *Journal of biomechanics*. 45. 1881-5. 10.1016/j.jbiomech.2012.05.031.
24. Kainz, H., Graham, D., Edwards, J., Walsh, H. P. J., Maine, S., Boyd, R. N., Lloyd, D. G., Modenese, L., & Carty, C. P. (2017). Reliability of four models for clinical gait analysis. *Gait & posture*, 54, 325–331.